

Dynamic fitness landscapes in the quasispecies model

Claus O. Wilke*, Christopher Ronnewinkel[†] and Thomas Martinetz[‡]
Institut für Neuro- und Bioinformatik
Medizinische Universität zu Lübeck
Seelandstr. 1a, 23569 Lübeck, Germany

December 4, 2018

Abstract

The quasispecies model is studied for the special case of externally varying replication rates. Most emphasis is laid on periodic time dependencies, but other cases are considered as well. For periodic time dependencies, the behavior of the evolving system can be determined analytically in several limiting cases. With that knowledge, the qualitative phase diagram in a given time-periodic fitness landscape can be predicted without almost any calculations. Several example landscapes are analyzed in detail in order to demonstrate the validity of this approach. For other, non-periodic time dependencies, it is also possible to obtain results in some of the limiting cases, so that there can be made predictions as well. Finally, the relationship between the results from the infinite population limit and the actual finite population dynamics is discussed.

*CO Wilke is on the leave to Caltech, Pasadena, CA. Email: claus.wilke@gmx.net

[†]C Ronnewinkel's current postal address is: Institut für Neuroinformatik, Ruhr-Universität Bochum 44780 Bochum, Germany. Email: ronne@neuroinformatik.ruhr-uni-bochum.de

[‡]Email: martinetz@informatik.mu-luebeck.de

Contents

1	Introduction	3
2	Time-dependent replication rates	5
3	Periodic fitness landscapes	8
3.1	Differential equation formalism	8
3.1.1	Neumann series for \mathbf{X}	9
3.1.2	Exact solutions for $R = 0$ and $R = 0.5$	12
3.1.3	Schematic phase diagrams	14
3.2	Discrete approximation	16
3.3	Example landscapes	17
3.3.1	One oscillating peak	17
3.3.2	Two oscillating peaks	21
3.3.3	Two oscillating peaks with flat average landscape	24
4	Aperiodic or stochastic fitness landscapes	27
5	Finite Populations	31
5.1	Numerical results	32
5.1.1	Loss of the master sequence	33
5.1.2	Persistency	35
5.2	A finite population on a simple periodic fitness landscape	36
5.2.1	The probability to skip one period	40
6	Conclusions	46
A	High-frequency expansion of $\mathbf{X}(t)$ for a landscape with two alternating master sequences	48

1 Introduction

Eigen’s quasispecies model [7] has been the basis of a vivid branch of molecular evolution theory ever since it has been put forward almost 30 years ago [31, 14, 12, 13, 8, 29, 17, 25, 15, 9, 28, 10, 20, 2, 36, 19, 3]. Its two main statements, the formation of a quasispecies made up of several molecular species with well defined concentrations, and the existence of an error threshold above which all information is lost because of accumulating erroneous mutations, have since then been observed in a large number of experimental as well as theoretical studies (see, e.g., [6] for the formation of a quasispecies in the RNA of the Q β phage, [1] for the observation of an error threshold in a system of self-replicating computer programs, and, generally, the reviews [9, 10, 3] and the references therein). Recently, a new aspect of the quasispecies model has been brought into consideration that was almost completely absent in previous works, namely the aspect of a dynamic fitness landscape [36, 19]. With the notion “dynamic fitness landscape”, we mean all situations in which the replication and/or decay rates of the molecules change over time. In the present work, we are only interested in situations where these changes occur as an external influence for the evolving system, and where there is no feedback from the system to the dynamics of the fitness landscape. Dynamic fitness landscapes of that kind are important, since almost any biological system is subject to external changes in the form of, e.g., daytime/nighttime, seasons, long-term climatic changes, geographic changes due to tectonic movements, to name just a few.

The main problem one encounters when dealing with dynamic landscapes is the difficulty to find a correct generalization of the quasispecies concept. In the original work of Eigen, the quasispecies is the equilibrium distribution of the different molecular species. It is reached if the system is left undisturbed for a sufficiently long time. Since in a dynamic landscape, the system is being disturbed by the landscape itself, the concept of a quasispecies is meaningless in the general case. However, there are special cases in which a meaningful quasispecies can be defined. If, for example, the landscape changes on a much slower time scale than what the system needs to reach the equilibrium, then the system is virtually in equilibrium all the time, and the concentrations at time t are determined from the landscape present at that time. Generally, certain symmetries in the dynamics of the landscape can allow for the definition of a quasispecies. One example we treat in this paper in detail is the case of time-periodic landscapes, which offer a natural quasispecies definition.

An early study of dynamic landscapes has been done by Jones [12, 13]. However, he has considered only cases in which all replication rates change by a common factor. Therefore, his approach excludes, among other cases, in particular

all situations in which the order of the molecules' replication rates changes over time, i.e., in which e.g. one of the faster replicating molecules becomes one of the slower replicating molecules and vice versa. The more recent work on dynamic fitness landscapes allow for such changes. Wilke *et al.* [35, 36] have developed a framework that allows to define and to calculate numerically a quasispecies in time-periodic landscapes. Independent of them, Nilsson and Snoad [19] have studied the particular example of a stochastically jumping peak in an otherwise flat landscape. This work has been generalized and refined by Ronnewinkel *et al.* [22], who could also define a meaningful quasispecies for a deterministic version of the jumping peak landscape and related landscapes. Finally, in the related field of genetic algorithms, there exist also some theoretical studies of dynamic fitness landscapes. Let us mention two of them. First of all, there is the work of Schmitt *et al.* [27, 26]. These authors derive results for finite populations (note that most results for the quasispecies model are only valid in the infinite population limit) in a relatively broad class of dynamic landscapes. However, they can only treat landscapes in which the fitnesses get scaled, so that the same restriction applies here that applied to Jone's work. The order of the fitnesses must never change. Second of all, Rowe [24, 23] has studied genetic algorithms with time-periodic landscapes. However, his approach has the caveat that it is tightly connected to the discrete time used in genetic algorithms, and that the dimension of the transition matrices grows in proportion to the period length T of the oscillation. This makes it hard to derive analytical results, and in addition to that, it renders landscapes with large T inaccessible to numerical calculations.

The remainder of this article is structured as follows. We begin our discussion in Section 2 with a brief summary of the general aspects of dynamic fitness landscapes in the quasispecies equation. In Section 3, we will develop the main subject of this work, a general theory of time-periodic fitness landscapes. The theoretical part thereof is presented in Section 3.1, in which we demonstrate how a time-dependent quasispecies can be defined by means of the monodromy matrix, and how this monodromy matrix can be expanded in terms of the oscillation period T . In Section 3.2, we present an alternative approximation formula for the monodromy matrix that is more suitable for numerical calculations, and in Section 3.3, we compare, for several example landscapes, the results obtained from that formula with the general theory developed in Section 3.1. The restriction of a time-periodic fitness landscape is weakened in Section 4, where we discuss the implications of our findings for other, non-periodic fitness landscapes. In that section, we are going to see that the qualitative results of the study of Nilsson and Snoad [19] are a direct consequence of the general theory for dynamic fitness landscapes. Since our work is based on Eigen's deterministic approach with differential equations, all results

presented up to the end of Section 4 are only valid for infinite population sizes. In order to address this shortcoming, in Section 5 we give a brief introduction into the problems involved when dealing with finite populations. In Section 5.1, some simulation results are shown, demonstrating the relationship between the results from the infinite population limit and the actual finite population dynamics. Finally, an approximative analytical description of a finite population evolving on a simple periodic landscape is developed in Section 5.2. We close this paper with some conclusions in Section 6.

2 Time-dependent replication rates

The quasispecies model describes the evolution of self-replicating macromolecules. It assumes that there exists only a finite number of different molecular species, and that each species i is present in high abundance, such that it suffices to record only the concentrations of the species, $x_i(t)$. The reaction dynamics is thought of taking place in a well-stirred reactor, with some constant out-flux of molecules $\bar{E}(t)$, such that the total concentration of molecules $\sum_i x_i(t)$ remains constant for all t . The self-replication process may fail, leading to erroneously copied offspring. This is being described by a mutation matrix Q_{ij} that gives the probability with which an offspring molecule of type i is generated from a parent j . Often, it is assumed that the molecules are RNA sequences, consisting of a string of letters A, G, C, U, or even simpler, the molecules are represented as bitstrings. In that case, one regularly makes the additional assumption that the replication process copies the string letter by letter, and that therefore the probability of a wrongly copied letter is independent of the letter's position in the string, and also of the type of the letter. In connection with that, it is useful to introduce the error rate per letter, R . In case we conceive the molecules of bitstrings of fixed length l , the mutation matrix Q_{ij} then takes on the form

$$Q_{ij} = (1 - R)^l \left(\frac{R}{1 - R} \right)^{d(i,j)}, \quad (1)$$

where $d(i, j)$ represents the Hamming distance between two sequences of type i and j . All our examples in later sections are based on that assumption. Our general results, however, do not depend on this assumption.

In vector notation, i.e. $\mathbf{x} = (x_1, x_2, \dots)$, the basic quasispecies equation reads

$$\dot{\mathbf{x}}(t) = [\mathbf{W}(t) - \bar{E}(t)\mathbf{1}]\mathbf{x}(t). \quad (2)$$

Here, $\mathbf{1}$ stands for the identity matrix, and $\mathbf{W}(t)$ is given by

$$\mathbf{W}(t) = \mathbf{Q}(t)\mathbf{A}(t) - \mathbf{D}(t), \quad (3)$$

where the diagonal matrix $\mathbf{A}(t)$ contains the replication coefficients, the diagonal matrix $\mathbf{D}(t)$ contains the decay constants, and the matrix $\mathbf{Q}(t)$ is the above introduced mutation matrix. In the most general case, all these three matrices can be time dependent. The average excess production can be expressed in terms of the matrices $\mathbf{A}(t)$ and $\mathbf{D}(t)$ as

$$\bar{E}(t) = \mathbf{e}^t \cdot [\mathbf{A}(t)\mathbf{x}(t) - \mathbf{D}(t)\mathbf{x}(t)], \quad (4)$$

where \mathbf{e}^t is a vector containing only entries of 1s, i.e. $\mathbf{e}^t = (1, \dots, 1)$.

Because of the $\mathbf{x}(t)$ dependence of $\bar{E}(t)$, Eq. (2) is nonlinear. However, as in the case of constant \mathbf{W} [31, 14], the introduction of new variables of the form

$$\mathbf{y}(t) = \exp\left(\int_0^t \bar{E}(\tau) d\tau\right) \mathbf{x}(t) \quad (5)$$

removes this nonlinearity. The resulting equation reads

$$\dot{\mathbf{y}}(t) = \mathbf{W}(t)\mathbf{y}(t), \quad (6)$$

and the concentrations can be obtained from $\mathbf{y}(t)$ via

$$\mathbf{x}(t) = \frac{\mathbf{y}(t)}{\mathbf{e}^t \cdot \mathbf{y}(t)}. \quad (7)$$

Note that if all decay constants are equal at all times, i.e. $\mathbf{D}(t) = \text{diag}(D(t), \dots, D(t))$, with a single scalar function $D(t)$, then an extended transformation

$$\mathbf{y}(t) = \exp\left(\int_0^t [\bar{E}(\tau) + D(t)] d\tau\right) \mathbf{x}(t) \quad (8)$$

leads to the even simpler equation

$$\dot{\mathbf{y}}(t) = \mathbf{Q}(t)\mathbf{A}(t)\mathbf{y}(t). \quad (9)$$

The concentration vector $\mathbf{x}(t)$ can again be obtained from Eq. (7).

The linearized quasispecies model, Eq. (6), has been studied in great detail for constant \mathbf{W} [9, 10]. Since the quasispecies is the equilibrium distribution of the molecular concentrations, the main question in that context has been the prediction of the system's behavior for $t \rightarrow \infty$. As a linear differential equation, Eq. (6) displays exponential growth [exponential damping does not occur because of the sign in front of the integral in Eq. (5)]. That growth may in principle be accompanied by exponentially amplified/damped oscillations. Of course, an equilibrium can only be defined if there are either no oscillations at all, or all

oscillations die out for $t \rightarrow \infty$. Fortunately, this is typically the case. First of all, for symmetric \mathbf{Q} , the whole spectrum of \mathbf{W} is real [25], because \mathbf{W} can be transformed into a symmetric matrix by means of a similarity transformation,

$$\mathbf{W} = \mathbf{QA} - \mathbf{D} \quad \rightarrow \quad \mathbf{A}^{1/2}\mathbf{WA}^{-1/2} = \mathbf{A}^{1/2}\mathbf{QA}^{1/2} - \mathbf{D}. \quad (10)$$

For non-symmetric \mathbf{Q} , we can apply the Frobenius-Perron theorem if the decay rates satisfy

$$(\mathbf{D})_{ii} < (\mathbf{QA})_{ii} \quad \text{for all } i. \quad (11)$$

The Frobenius-Perron theorem guarantees a real largest eigenvalue. Consequently, we have at most exponentially damped oscillations as long as we obey (11). In addition to that, the Frobenius-Perron theorem states that the eigenvector corresponding to this largest eigenvalue has only strictly positive entries, and hence, that this eigenvector can be interpreted as a vector of chemical concentrations if normalized appropriately.

Now consider the case of a full time dependency. In that case, we can map the quasispecies model onto a linear system with a symmetric matrix $\tilde{\mathbf{W}}(t)$ if $\mathbf{Q}(t)$ is symmetric for all t . This can be seen by introducing

$$\mathbf{z}(t) = \mathbf{A}^{1/2}(t)\mathbf{y}(t). \quad (12)$$

Differentiation yields

$$\dot{\mathbf{z}}(t) = \tilde{\mathbf{W}}(t)\mathbf{z}(t) \quad (13)$$

$$\text{with } \tilde{\mathbf{W}}(t) = \mathbf{A}^{1/2}(t)\mathbf{Q}(t)\mathbf{A}^{1/2}(t) - \mathbf{D}(t) + \left[\frac{d}{dt}\mathbf{A}^{1/2}(t) \right] \mathbf{A}^{-1/2}(t). \quad (14)$$

Nevertheless, we cannot write down a solution for Eq. (13) from the knowledge of the eigensystem of $\tilde{\mathbf{W}}(t)$ if $\tilde{\mathbf{W}}(t)$ has an arbitrary time dependency. Therefore, the symmetric quasispecies equation (13) does not help us in solving Eq. (6). As a consequence, we have to focus on limiting cases for which general statements can be made. The two most important limiting cases are very fast changes in $\mathbf{W}(t)$ on the one hand, and very slow changes in $\mathbf{W}(t)$ on the other hand. We begin with the case of very slow changes. For the rest of this work, we will assume that $\mathbf{W}(t)$ has a real spectrum for all t . From Eq. (13), we know that this covers at least all cases for which $\mathbf{Q}(t)$ is symmetric. To be on the safe side, we also assume that (11) is satisfied for all t . In that way, the Perron eigenvector of $\mathbf{W}(t)$ can always be interpreted as a vector of chemical concentrations.

For every time t_0 , we can define a relaxation time

$$\tau_{\text{R}}(t_0) = \frac{1}{\lambda_0(t_0) - \lambda_1(t_0)}, \quad (15)$$

where $\lambda_0(t_0)$ and $\lambda_1(t_0)$ are the largest and the second largest eigenvalue of $\mathbf{W}(t_0)$, respectively. The time $\tau_{\text{R}}(t_0)$ gives an estimate on how long a linear system with matrix $\mathbf{W}(t_0)$ needs to settle into equilibrium. Therefore, if the changes in $\mathbf{W}(t)$ happen on a timescale much longer than $\tau_{\text{R}}(t)$, the system is virtually in equilibrium at any given point in time. Hence, for large enough t , the quasispecies will be given by the Perron eigenvector of $\mathbf{W}(t)$. Strictly speaking, this is only true if there is always some overlap between the largest eigenvector of $\mathbf{W}(t)$ and the one of $\mathbf{W}(t + dt)$, but in all but some very pathological cases we can assume this to be the case.

The situation of fast changes in $\mathbf{W}(t)$ is somewhat more difficult, because, as we are going to see later on, we have to define a suitable average over $\mathbf{W}(t)$ in order to make a general statement. Therefore, we postpone that situation for a moment. A detailed discussion of fast changes will be given for the particular case of periodic fitness landscapes in the next section, and later on, we will discuss fast changing landscapes in general.

3 Periodic fitness landscapes

3.1 Differential equation formalism

In this section, we are going to study periodic time dependencies in $\mathbf{W}(t)$, for which we can demonstrate several general statements.

If the changes in $\mathbf{W}(t)$ are periodic, i.e., if there exists a T such that

$$\mathbf{W}(t + T) = \mathbf{W}(t) \quad \text{for all } t, \quad (16)$$

then Eq. (6) turns into a system of linear differential equations with periodic coefficients. Several theorems are known for such systems [37]. Most notably, if $\mathbf{Y}(t, t_0)$ is the fundamental matrix, such that every solution to Eq. (6) can be written in the form

$$\mathbf{y}(t) = \mathbf{Y}(t, t_0)\mathbf{y}(t_0), \quad (17)$$

then we can define a so-called monodromy matrix $\mathbf{X}(t_0)$,

$$\mathbf{X}(t_0) = \mathbf{Y}(t_0 + T, t_0), \quad (18)$$

which simplifies Eq. (17) to

$$\begin{aligned}\mathbf{y}(t) &= \mathbf{Y}(t_0 + \phi, t_0)\mathbf{X}^m(t_0)\mathbf{y}(t_0) \\ &= \mathbf{X}^m(t_0 + \phi)\mathbf{Y}(t_0 + \phi, t_0)\mathbf{y}(t_0),\end{aligned}\tag{19}$$

for the decomposition $t = mT + \phi + t_0$ with the phase $\phi < T$. In particular, we have

$$\mathbf{y}(\phi + mT) = \mathbf{X}^m(\phi)\mathbf{y}(\phi),\tag{20}$$

so that for every phase ϕ , we have a well defined asymptotic solution, given by the eigenvector to the largest eigenvalue of $\mathbf{X}(\phi)$. In other words, periodic fitness landscapes allow the definition of a quasispecies, much in the same way as static fitness landscapes do. However, this quasispecies is time-dependent, and the time-dependency is periodic with period T .

3.1.1 Neumann series for \mathbf{X}

We can derive a formal expansion in T for the monodromy matrix. This formal expansion is similar in spirit to the Neumann series which gives a formal solution to an integral equation, and it is based on the Picard-Lindelöf iteration for differential equations. As the first step, we have to rewrite Eq. (6) in the form of an integral equation, i.e.

$$\mathbf{y}(t_0 + \tau) = \mathbf{y}(t_0) + \int_0^\tau \mathbf{W}(t_0 + \tau_1)\mathbf{y}(t_0 + \tau_1)d\tau_1.\tag{21}$$

Our goal is to solve this equation for $\mathbf{y}(t_0 + \tau)$ by iteration. Our initial solution is

$$\mathbf{y}_0(t_0 + \tau) = \mathbf{y}(t_0),\tag{22}$$

which we insert into Eq. (21). As a result, we obtain the 1st order approximation

$$\mathbf{y}_1(t_0 + \tau) = \mathbf{y}(t_0) + \int_0^\tau \mathbf{W}(t_0 + \tau_1)\mathbf{y}(t_0)d\tau_1.\tag{23}$$

Further iteration yields

$$\begin{aligned}\mathbf{y}_2(t_0 + \tau) &= \mathbf{y}(t_0) + \int_0^\tau \mathbf{W}(t_0 + \tau_1)\mathbf{y}(t_0)d\tau_1 \\ &\quad + \int_0^\tau \mathbf{W}(t_0 + \tau_1) \int_0^{\tau_1} \mathbf{W}(t_0 + \tau_2)\mathbf{y}(t_0)d\tau_2d\tau_1,\end{aligned}\tag{24}$$

and so on. Now we define

$$\overline{\mathbf{W}}_0(t_0, \tau) = 1, \quad (25)$$

$$\overline{\mathbf{W}}_1(t_0, \tau) = \frac{1}{\tau} \int_0^\tau \mathbf{W}(t_0 + \tau_1) d\tau_1, \quad (26)$$

and, in general

$$\overline{\mathbf{W}}_k(t_0, \tau) = \frac{1}{\tau^k} \int_0^\tau \mathbf{W}(t_0 + \tau_1) \int_0^{\tau_1} \mathbf{W}(t_0 + \tau_2) \cdots \int_0^{\tau_{k-1}} \mathbf{W}(t_0 + \tau_k) d\tau_1 d\tau_2 \cdots d\tau_k, \quad (27)$$

and obtain the formal solution

$$\mathbf{y}(t_0 + \tau) = \sum_{k=0}^{\infty} \tau^k \overline{\mathbf{W}}_k(t_0, \tau) \mathbf{y}(t_0). \quad (28)$$

For suitably small τ , the infinite sum on the right-hand side is guaranteed to converge. When we compare this equation for $\tau = T$ to the definition of the monodromy matrix Eq. (18), we find that [introducing $\overline{\mathbf{W}}_k(t_0) := \overline{\mathbf{W}}_k(t_0, T)$]

$$\mathbf{X}(t_0) = \sum_{k=0}^{\infty} T^k \overline{\mathbf{W}}_k(t_0). \quad (29)$$

In particular, since $\overline{\mathbf{W}}_1(t_0)$ is identical to the time-average over $\mathbf{W}(t)$, regardless of t_0 , we have the high-frequency expansion

$$\mathbf{X}(t_0) = \mathbf{1} + T \overline{\mathbf{W}} + \mathcal{O}(T^2), \quad (30)$$

with

$$\overline{\mathbf{W}} = \frac{1}{T} \int_0^T \mathbf{W}(t) dt. \quad (31)$$

Equation (30) reveals that for very high frequency oscillations, the system behaves as being in a static landscape. That static landscape is given by the dynamic landscape's average over one oscillation period.

The radius of convergence of the expansion Eq. (29) can be estimated as follows. Since all entries of $\mathbf{W}(t)$ are positive, we have for the tensor

$$\begin{aligned} \overline{W}_{i\nu_1} \overline{W}_{\nu_1\nu_2} \cdots \overline{W}_{\nu_{k-1}j}(t_0) &:= \frac{1}{T^k} \int_0^T W_{i\nu_1}(t_0 + \tau_1) \int_0^{\tau_1} W_{\nu_1\nu_2}(t_0 + \tau_2) \\ &\cdots \int_0^{\tau_{k-1}} W_{\nu_{k-1}j}(t_0 + \tau_k) d\tau_1 d\tau_2 \cdots d\tau_k \end{aligned} \quad (32)$$

the estimate

$$\overline{W}_{i\nu_1} \overline{W}_{\nu_1\nu_2} \cdots \overline{W}_{\nu_{k-1}j}(t_0) \leq \frac{1}{T^k} \int_0^T W_{i\nu_1}(t_0 + \tau) d\tau \int_0^T W_{\nu_1\nu_2}(t_0 + \tau) d\tau \cdots \int_0^T W_{\nu_{k-1}j}(t_0 + \tau) d\tau, \quad (33)$$

from which follows

$$(\overline{\mathbf{W}}_k(t_0))_{ij} \leq (\overline{\mathbf{W}}^k)_{ij}. \quad (34)$$

The matrix norm induced by the sum norm

$$\|(y_1, y_2, \dots, y_n)\|_1 = \sum_i |y_i| \quad (35)$$

is the column-sum norm

$$\|\overline{\mathbf{W}}\|_1 = \max_j \left\{ \sum_i |\overline{W}_{ij}| \right\}. \quad (36)$$

With that norm, we can with the aid of Eq. (34) estimate

$$\|\overline{\mathbf{W}}_k(t_0)\|_1 \leq \|\overline{\mathbf{W}}^k\|_1 \leq \|\overline{\mathbf{W}}\|_1^k. \quad (37)$$

Hence, the expansion Eq. (29) converges certainly for those T that satisfy

$$T \|\overline{\mathbf{W}}\|_1 < 1. \quad (38)$$

Since all entries in \mathbf{W} are positive, we have further

$$\begin{aligned} \|\overline{\mathbf{W}}\|_1 &= \max_j \left\{ \sum_i |\overline{A}_j Q_{ij} - \overline{D}_j \delta_{ij}| \right\} \\ &= \max_j \{ \overline{A}_j - \overline{D}_j \}, \end{aligned} \quad (39)$$

where the bar in \overline{A}_j and \overline{D}_j indicates that these quantities represent averages over one oscillation period. The second equality holds because of (11) and because of $\sum_i Q_{ij} = 1$. Without loss of generality, we assume that the maximum is given by $\overline{A}_0 - \overline{D}_0$. Then, Eq. (38) is satisfied for

$$T < \frac{1}{\overline{A}_0 - \overline{D}_0}. \quad (40)$$

It is interesting to compare this expression to the relaxation time of the time-averaged fitness landscape, $\bar{\tau}_R$. To 0th order, the principal eigenvalue of $\bar{\mathbf{W}}$ is given by \bar{W}_{00} . The second largest eigenvalue is to the same order given by the second largest diagonal element of $\bar{\mathbf{W}}$, which we assume to be \bar{W}_{11} without loss of generality. Hence, the relaxation time is approximately given by

$$\bar{\tau}_R = \frac{1}{\bar{W}_{00} - \bar{W}_{11}} > \frac{1}{\bar{W}_{00}} \geq \frac{1}{\bar{A}_0 - \bar{D}_0}, \quad (41)$$

which is generally larger than the radius of convergence of Eq. (29). In particular, if the largest and the second largest eigenvalue of $\bar{\mathbf{W}}$ lie close together, the relaxation time may be much larger than the largest oscillation period for which the expansion is feasible. This restricts the usability of Eq. (29) to considerably high frequency oscillations in the landscape. The interesting regime in which the changes in the landscape happen on a time scale comparable to the relaxation time of the system can unfortunately not be studied from Eq. (29).

3.1.2 Exact solutions for $R = 0$ and $R = 0.5$

The two extreme cases $R = 0$ (no replication errors) and $R = 0.5$ (random offspring sequences) allow for an exact analytic treatment. The second case is identical to the situation in static landscapes, and therefore we will mention it only briefly. At the point of stochastic replication $R = 0.5$, the population dynamics becomes independent of the details of the landscape. As a consequence, temporal changes in the landscape must become less important as R approaches $R = 0.5$. However, this is not very surprising, since in most cases, an error rate close to 0.5 implies that the population has already passed the error threshold, which in turn implies that it does not feel the changes in the landscape any more.

The case of $R = 0$, on the other hand, is more complex than the corresponding case in a static landscape. Since the matrix \mathbf{Q} becomes the identity matrix for $R = 0$, Eq. (6) reduces to

$$\dot{\mathbf{y}}(t) = [\mathbf{A}(t) - \mathbf{D}(t)]\mathbf{y}(t). \quad (42)$$

The matrices $\mathbf{A}(t)$ and $\mathbf{D}(t)$ are diagonal by definition, and hence, a solution to Eq. (42) is given by

$$\mathbf{y}(t) = \exp\left(\int_{t_0}^t [\mathbf{A}(t') - \mathbf{D}(t')]dt'\right)\mathbf{y}(t_0). \quad (43)$$

When we compare this expression to Eqs. (17) and (18), we find

$$\mathbf{Y}(t, t_0) = \exp\left(\int_{t_0}^t [\mathbf{A}(t') - \mathbf{D}(t')]dt'\right), \quad (44)$$

and, in particular,

$$\mathbf{X}(\phi) = \exp\left(\int_{\phi}^{\phi+T} [\mathbf{A}(t') - \mathbf{D}(t')] dt'\right). \quad (45)$$

The integral in the second expression is taken over a complete oscillation period, and hence, it is independent of ϕ . Thus, we find for arbitrary ϕ

$$\mathbf{X}(\phi) = \exp(\overline{\mathbf{W}}) \quad \text{for } R = 0. \quad (46)$$

With a vanishing error rate, the monodromy matrix becomes the exponential of the time-average over $\mathbf{W}(t)$. Since the exponential function only affects the eigenvalues, but not the eigenvectors, of a matrix, the quasispecies is given by the principal eigenvector of $\overline{\mathbf{W}}$, irrespective of the length of the oscillation period T . In other words, under the absence of mutations will the sequence i with the highest average value of $A_i(t) - D_i(t)$ take over the whole population after a suitable amount of time, provided it existed already in the population at the beginning of the process. By continuity, this property must extend to very small but positive error rates R . So, similar to the case of $R = 0.5$, the temporal changes in the landscape lose their importance when R approaches 0.

There is, however, a caveat to the above argument. In case the largest eigenvalue of $\overline{\mathbf{W}}$ is degenerate, temporal changes in the landscape may continue to be of importance for $R = 0$. A degeneracy of the largest eigenvalue of $\overline{\mathbf{W}}$ is possible, because the Frobenius-Perron theorem applies only to positive error rates. For degenerate quasispecies, the initial condition $\mathbf{y}(t_0)$ determines the composition of the asymptotic population. In this context, let us consider the general solution for periodic fitness landscapes, Eq. (19). We have

$$\mathbf{y}(t) = \mathbf{X}^m(\phi)\mathbf{y}(t_0 + \phi) \quad (47)$$

with

$$\mathbf{y}(t_0 + \phi) = \mathbf{Y}(t_0 + \phi, t_0)\mathbf{y}(t_0). \quad (48)$$

So even if \mathbf{X} becomes independent of ϕ for $R = 0$, this need not be the case for $\mathbf{y}(t_0 + \phi)$, because of Eq. (48). If the largest eigenvalue of $\overline{\mathbf{W}}$ is degenerate, these variations in $\mathbf{y}(t_0 + \phi)$ will remain visible for arbitrarily large times t . Hence, we will see oscillations among the different quasispecies which correspond to the largest eigenvalue. Clearly, this effect is the more pronounced the larger the oscillation period T .

3.1.3 Schematic phase diagrams

The results of the previous two subsections allow us to identify the general properties of the quasispecies model with a periodic fitness landscape at the borders of the parameter space. We have to consider only the two parameters error rate R and oscillation period T , since all other parameters (replication rates, decay rates, details of the matrix \mathbf{Q}) do not influence the above results. In Fig. 1, we have summarized our findings. Along the abscissa runs the oscillation period. For very fast oscillations, the evolving population sees only the time-averaged landscape. For very slow oscillations, on the other hand, the population is able to settle into an equilibrium much faster than the changes in the landscape occur. Hence, the population sees a quasistatic landscape. Along the ordinate, we have displayed the error rate. For the error rate, we have disregarded the region above $R = 0.5$, in which anti-correlations between parent and offspring sequences are present. For $R = 0.5$, all sequences have random offspring, and hence, all sequences replicate equally well. Therefore, for this error rate, the landscape becomes effectively flat. On the other side, for $R = 0$, we have again the time-averaged landscape. However, for large T , the fact that we see the average landscape does not mean that the concentration variables are asymptotically constant. Degeneracies in the largest eigenvalue may cause a remaining time dependency due to oscillations between superposed quasispecies. The exact form of these oscillations is dependent on the initial condition $\mathbf{y}(0)$. For small T , the oscillations disappear, because the ratio of newly created sequences during one oscillation period and remaining sequences from the previous oscillation period decays with T [Eq. (30)].

From the above observations, we can derive generic phase diagrams for periodic fitness landscapes. There are two main possibilities. The fitness landscape may average to a landscape that has a distinct quasispecies, or it may average to a flat landscape. These two cases are illustrated in Fig. 2. Note that the diagrams are meant to illustrate the qualitative form and position of the different phases. In their exact appearance, they may differ substantially from the exact phase diagram of a particular landscape.

If a landscape averages to one with a distinct quasispecies, then for every oscillation period T and every phase of the oscillation ϕ , we have a unique error threshold $R^*(T, \phi)$. For small T , the error threshold converges towards the one of the average fitness landscape, R_{av}^* , irrespective of the phase ϕ . For larger T , the error threshold oscillates between $R_{\text{lo}}^* = \min_{\phi} R^*(T, \phi)$ and $R_{\text{hi}}^* = \max_{\phi} R^*(T, \phi)$. In the limit of an infinitely large oscillation period, R_{hi}^* converges towards R_{max}^* , which is the largest error threshold of all the (static) landscapes $\mathbf{W}(\phi)$. Similarly, R_{lo}^* converges towards R_{min}^* in that limit, where R_{min}^* is accordingly defined as the smallest error threshold of all landscapes $\mathbf{W}(\phi)$. For a fixed oscillation period T ,

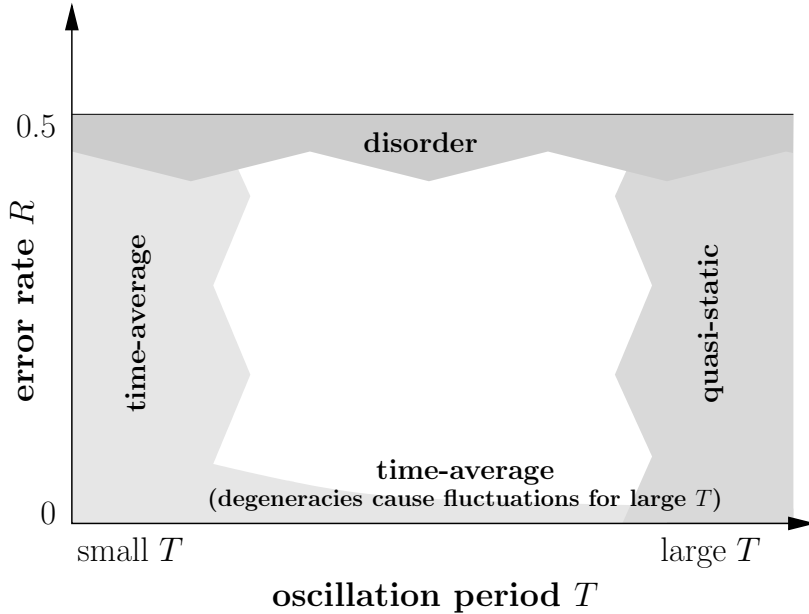


Figure 1: The appearance of a periodic fitness landscape at the border regions of the parameter space.

and a fixed error rate R with $R_{lo}^* < R < R_{hi}^*$, we have necessarily $R > R^*(T, \phi)$ for some phases ϕ , and $R < R^*(T, \phi)$ for the rest of the oscillation period. As a result, a quasispecies will form whenever $R > R^*(T, \phi)$, but it will disappear again as soon as $R < R^*(T, \phi)$. This phenomenon has for the first time been observed in [36], and there, the region of the parameter space in which it can be found has been called the *temporarily ordered phase*. In this phase, whether we observe order or disorder depends on the particular moment in time at which we study the system. In correspondence to that, we will call a phase “ordered” only if order can be seen for the whole oscillation period, and we will call a phase “disordered” if during the whole oscillation period no order can be seen. The relationship between the ordered phase, the disordered phase, and the temporarily ordered phase for the first type of landscapes is displayed in Fig. 2a). Compare also the phase diagram of the oscillating Swetina-Schuster landscape in Fig. 3.

In a landscape that averages to a flat one, on the other hand, the disordered phase must extend over the whole range of R for sufficiently small T . Order can be observed only above a certain T_{min} . However, slightly above that T_{min} , no order will be found for error rates R other than intermediate ones, since for $R = 0$ the landscape averages again to a flat one. Hence, what we will observe is an ordered or temporarily ordered phase restricted from above and from below. Instead of a

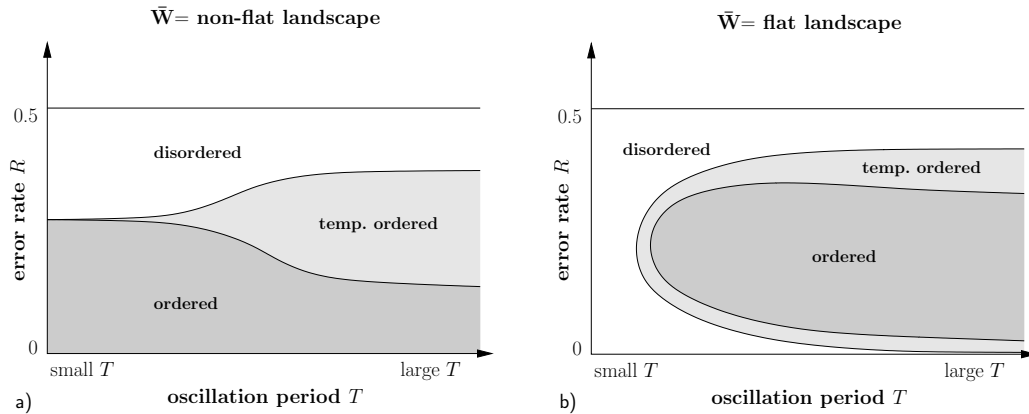


Figure 2: The two possible phase diagrams of a periodic landscape. If $\mathbf{W}(t)$ averages to a non-flat landscape, there will typically be a lower error threshold, below which we always find order, and a higher error threshold, above which the system is always in a disordered state. If $\mathbf{W}(t)$ averages to a flat landscape, however, the disordered phase extends to the whole range of R for sufficiently small T .

unique error threshold $R^*(T, \phi)$, we have for every phase ϕ a lower threshold that marks the transition from disorder to order, and a higher threshold that marks the transition back to disorder. For longer oscillation periods, the fluctuations in the degenerate quasispecies become important for $R = 0$, and this fact allows the ordered regime to extend to much smaller values of R . Hence, the lower disordered phase will fade out for $T \rightarrow \infty$. A typical phase diagram for this type of landscapes is displayed in Fig. 2b).

3.2 Discrete approximation

The differential equation formalism we have used so far allows for an elegant discussion of the system's general properties. However, if we want to obtain numerical solutions, this formalism does not help us very much, because we do not have a general expression for the fundamental matrix $\mathbf{Y}(t, t_0)$ from Eq. (17), nor for the monodromy matrix $\mathbf{X}(t_0)$ from Eq. (18). Therefore, for our numerical treatment we will move over to the discretized quasispecies equation,

$$\mathbf{y}(t + \Delta t) = [\Delta t \mathbf{W}(t) + \mathbf{1}] \mathbf{y}(t). \quad (49)$$

In the case of constant \mathbf{W} , the quasispecies obtained from that equation is identical to the one of Eq. (6), and it is also identical to the one of the equation

$$\mathbf{y}(t + 1) = \mathbf{W} \mathbf{y}(t). \quad (50)$$

Equation (50) has been studied by Demetrius *et al.* [4], and has been employed by Leuthäusser [15] for her mapping of the quasispecies model onto the Ising model. In the general time-dependent case, however, the additional factor Δt and the identity matrix $\mathbf{1}$ of Eq. (49) are important, and cannot be left out. The analogue of the fundamental matrix for Eq. (49) reads

$$\mathbf{Y}(t_0 + k\Delta t, t_0) = \mathcal{T} \left\{ \prod_{\nu=0}^{k-1} [\Delta t \mathbf{W}(t_0 + \nu\Delta t) + \mathbf{1}] \right\}, \quad (51)$$

where $\mathcal{T}\{\cdot\}$ indicates that the matrix product has to be evaluated with the proper time ordering [35]. Similarly, the analogue of the monodromy matrix becomes

$$\begin{aligned} \mathbf{X}(t_0) &= \mathbf{Y}(t_0 + T, t_0) \\ &= \mathcal{T} \left\{ \prod_{\nu=0}^{n-1} [\Delta t \mathbf{W}(t_0 + \nu\Delta t) + \mathbf{1}] \right\}, \end{aligned} \quad (52)$$

where we have assumed that T is an integral multiple of Δt , and have set $n = T/\Delta t$. The influence of the size of Δt on the quality of the approximation has been investigated in [35]. A more in-depths discussion of the relationship between the continuous and the discrete quasispecies model can also be found in [3].

3.3 Example landscapes

For the rest of this section, we are going to have a look at several example landscapes, in order to illustrate the implications of our general theory. In all cases considered, we represent the molecules as bitstrings of fixed length l . Moreover, we assume that a single bit is copied erroneously with rate R , irrespective of the bit's type and of its position in the string.

3.3.1 One oscillating peak

In the previous works on the quasispecies model with periodic fitness landscapes [35, 36], most emphasis has been laid on landscapes with a single oscillating sharp peak. As a generalization of the work of Swetina and Schuster [29], the master sequence has been given a replication rate $A_0(t) \gg A$, where A is the replication rate of all other sequences. The replication rate $A_0(t)$ has been expressed as

$$A_0(t) = A_{0,\text{stat}} \exp[\epsilon f(t)], \quad (53)$$

with a T -periodic function $f(t)$. The parameter ϵ allows a smooth crossover from a static landscape to one with considerable dynamics, and the exponential assures

that $A_0(t)$ is always positive. In order not to duplicate work, we will not repeat the results of [35, 36] here. In short, it has been found that the behavior at the border regions of the parameter space is indeed as it is depicted in Fig. 1, and that a phase diagram of the form of Fig. 2a) correctly describes the relationship of order and disorder in an oscillating Swetina-Schuster landscape. Here, our aim is to show that the phase borders in such a phase diagram can, for an oscillating Swetina-Schuster landscape, be calculated approximately.

For static landscapes with a single peak, the assumption of a vanishing mutational backflow into the master sequence allows to derive an approximate expression for the error threshold [16, 9, 10]. A similar formula can be developed to calculate the error threshold as a function of time in a landscape with a single oscillating peak. But before we turn towards the dynamic landscape, we are going to rederive the expression for the master's concentration x_0 in a static landscape, based on the neglect of mutational backflow. The expression we are going to find is slightly more general than the one that was previously given, and it will be of use for the periodic fitness landscape as well.

The 0th component of the quasispecies equation (2) becomes, after neglecting the mutational backflow,

$$\dot{x}_0(t) = W_{00}x_0(t) - \bar{E}(t)x_0(t). \quad (54)$$

The average excess production $\bar{E}(t)$ can be expressed in terms of $\mathbf{x}(t)$ and \mathbf{W} as

$$\bar{E}(t) = \sum_{i,j} W_{ij}x_j(t). \quad (55)$$

With that expression, the solution of Eq. (54) requires the knowledge of the stationary mutant concentrations x_j , which are usually unknown. To circumvent this problem, we make the somewhat extreme assumption that all mutant concentrations are equal. Although this assumption, which is equivalent to the assumption of equal excess productions E_i in the usual calculation without mutational backflow, will generally not be true, it works fine for Swetina-Schuster type landscapes. With this additional assumption, Eq. (55) becomes

$$\bar{E}(t) = \sum_i \left[\sum_{j>0} W_{ij} \frac{1 - x_0(t)}{N - 1} + W_{i0}x_0(t) \right], \quad (56)$$

where N is the number of different sequences in the system. When we insert this into Eq. (54) and solve for the steady state, we find

$$x_0 = \frac{W_{00} - \frac{1}{N-1} \sum_i \sum_{j>0} W_{ij}}{\sum_i W_{i0} - \frac{1}{N-1} \sum_i \sum_{j>0} W_{ij}}. \quad (57)$$

The expressions involving sums over matrix elements in Eq. (57) can be identified with the excess production of the master,

$$E_0 = \sum_i W_{i0} \quad (58)$$

and with the average excess production without the master,

$$\bar{E}_{-0} = \frac{1}{N-1} \sum_i \sum_{j>0} W_{ij}, \quad (59)$$

if \mathbf{W} has the standard form $\mathbf{QA} - \mathbf{D}$. Therefore, Eq. (57) corresponds to the often quoted result

$$x_0 = \frac{W_{00} - \bar{E}_{-0}}{E_0 - \bar{E}_{-0}}. \quad (60)$$

However, Eq. (57) is more general in that it can be used even if \mathbf{W} is not given as $\mathbf{QA} - \mathbf{D}$.

Our idea here is to insert the monodromy matrix into Eq. (57) in order to obtain an approximation for x_0 in the case of periodic landscapes. But why can we expect this to work? After all, Eq. (57) has been derived from an equation with continuous time, Eq. (54), whereas the monodromy matrix advances the system in discrete time steps, as can be seen in Eq. (20). The important point is here that we are only interested in the asymptotic state, which is given by the normalized Perron vector of the monodromy matrix, whether we use discrete or continuous time. Therefore, we are free to calculate the asymptotic state in a periodic landscape for a given phase ϕ from

$$\dot{\mathbf{y}}(t) = \mathbf{X}(\phi)\mathbf{y}(t), \quad (61)$$

even if this equation does not have a direct physical meaning for finite times. The asymptotic molecular concentrations are then given by the limit $t \rightarrow \infty$ of

$$\mathbf{x}(t) = \frac{\mathbf{y}(t)}{\mathbf{e} \cdot \mathbf{y}(t)}. \quad (62)$$

From differentiating Eq. (62) and inserting Eq. (61), we obtain

$$\dot{\mathbf{x}}(t) = \mathbf{X}(\phi)\mathbf{x}(t) - \mathbf{x}(t)(\mathbf{e} \cdot [\mathbf{X}(\phi)\mathbf{x}(t)]). \quad (63)$$

When we neglect the backflow onto the master sequence, the 0th component of that equation becomes identical to Eqs. (54) and (55), but with the matrix $\mathbf{X}(\phi)$

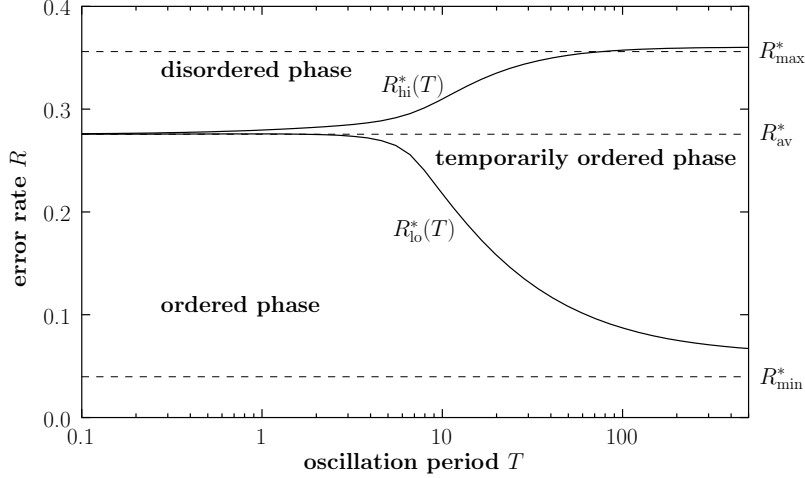


Figure 3: The phase diagram of an oscillating Swetina-Schuster landscape [$A_0(t) = e^{2.4} \exp(2 \sin \omega t)$], numerically calculated from Eq. (57).

instead of \mathbf{W} . This shows that we may indeed use Eq. (57) as an approximation for the asymptotic concentration of x_0 . Of course, since we have neglected mutational backflow, this approximation works only for landscapes in which a single sequence has a significant advantage over all others. But this restriction does similarly apply to the static case. Numerically, we have found that Eq. (57) works well for a single oscillating peak, and that it breaks down in other cases as expected.

With the aid of Eq. (57), we are now in the position that we can calculate the phase diagram of the oscillating Swetina-Schuster landscape. When we insert the monodromy matrix $\mathbf{X}(\phi)$ into Eq. (57), we are able to obtain (numerically) the error rate at which x_0 vanishes, $R^*(T, \phi)$. From that expression, we can calculate R_{lo}^* and R_{hi}^* . The results of the corresponding, numerically extensive calculations are shown in Fig. 3, together with R_{av}^* , R_{max}^* , and R_{min}^* , which have also been determined from Eq. (57).

We find that both R_{lo}^* and R_{hi}^* approach R_{av}^* for $T \rightarrow 0$, as predicted by our general theory. For $T \rightarrow \infty$, R_{hi}^* grows quickly to the level of R_{max}^* , but a slight discrepancy between the two values remains. It has its origin in the vast complexity of the numerical calculations involved for large T . We can only approximate the monodromy matrix by means of Eq. (52), and we need ever more factors $\Delta t \mathbf{W}(t_0 + \nu \Delta t) + \mathbf{1}$ for large T . The discrepancy between R_{lo}^* and R_{min}^* , on the other hand, has a different origin. The main cause here is the fact that the relaxation into equilibrium is generally slower for smaller error rates. Therefore, R_{lo}^* needs a much larger T to reach R_{min}^* than it is the case with R_{hi}^* and R_{max}^* .

3.3.2 Two oscillating peaks

A single oscillating peak provides some initial insights into dynamic fitness landscapes. It is more interesting, however, to study situations in which several sequences obtain the highest replication rate in different phases of the oscillation period. The simplest such case is a landscape in which two sequences become in turn the master sequence. Here, we will assume that the two are located at opposite corners of the boolean hypercube, i.e., that they are given by a certain sequence and its inverse. In that way, it is possible to group sequences into error classes according to their Hamming distance to one of the two possible master sequences. As an example, we are going to study a landscape with the replication coefficients

$$A_0(t) = A_{0,\text{stat}} \exp(\epsilon \sin \omega t), \quad (64a)$$

$$A_l(t) = A_{0,\text{stat}} \exp(-\epsilon \sin \omega t), \quad (64b)$$

$$A_i(t) = 1 \quad \text{for } 0 < i < l. \quad (64c)$$

The subscripts in the replication coefficients stand for the Hamming distance to the sequence $000 \dots 0$.

For single peak landscapes, it is instructive to characterize the state of the system at time t by the value of the order parameter

$$m_s(t) = \frac{1}{l} \sum_{i=0}^l x_i(t) [l - 2i], \quad (65)$$

where $x_i(t)$ is the cumulative concentration of all sequences of Hamming distance i to the master sequence [15, 30]. If the master sequence makes up the whole population, we have $m_s(t) = 1$. A completely disordered population, on the other hand, yields $m_s(t) = 0$. In principle, $m_s(t)$ can also be used for a landscape with two alternating master sequences if they are each other's inverse. In that case, the Hamming distance has to be measured with respect to one of the two master sequences. If the population consists only of sequences of the type of the other master sequence, we have $m_s(t) = -1$. However, there is a small problem with degenerate landscapes, in which the two peaks have the same replication rate. In such landscapes, the sequence distribution becomes symmetric with respect to the two peaks, i.e., $x_0 = x_l$, $x_1 = x_{l-1}$, and so on. Then, $m_s(t)$ becomes zero because of this symmetry, although the population may be in an ordered state. To distinguish between the case of true disorder and the case of an ordered, but

symmetrical population, we introduce the additional order parameters

$$m_s^+(t) = \frac{1}{l} \sum_{i=0}^{\lfloor (l-1)/2 \rfloor} x_i(t)[l-2i], \quad (66)$$

and

$$m_s^-(t) = \frac{1}{l} \sum_{i=l-\lfloor (l-1)/2 \rfloor}^l x_i(t)[l-2i]. \quad (67)$$

Here, $\lfloor x \rfloor$ stands for the largest integer smaller than or equal to x .

The quantity $m_s^+(t)$ is always positive, $m_s^-(t)$ is always negative, and furthermore, we have

$$m_s(t) = m_s^+(t) + m_s^-(t). \quad (68)$$

If the population is uniformly distributed over the whole sequence space, we have

$$m_s^+(t) = -m_s^-(t) = \frac{1}{l2^l} \sum_{i=0}^{\lfloor (l-1)/2 \rfloor} \binom{l}{i} (l-2i). \quad (69)$$

This expression goes to 0 for $l \rightarrow \infty$. If, on the other hand, only the two peaks are populated, each with half of the total population, we find

$$m_s^+(t) = -m_s^-(t) = \frac{1}{2}. \quad (70)$$

In the case that either $m_s^+(t)$ or $m_s^-(t)$ equal to zero, the population is centered about the respective other peak.

In the following, when it is important to distinguish between true disordered populations and symmetric populations, we will use $m_s^+(t)$ and $m_s^-(t)$. When the situation is non-ambiguous, we will use $m_s(t)$ alone, in order to improve the clarity of our plots.

In Fig. 4, we have displayed $m_s^+(t)$, $m_s^-(t)$ and $m_s(t)$ for the quasispecies in a fitness landscape of the type defined in Eq. (64). For a large oscillation period, $T = 100$, the quasispecies is at every point in time clearly centered around a single peak. The switch from one peak to the other happens very fast. When the landscape oscillates with a higher frequency, the transition time uses up a larger proportion of the total oscillation period. This makes the transition from one peak to the other appear softer in the plots for smaller oscillation periods. For extremely small oscillations, the system sees the average fitness landscape,

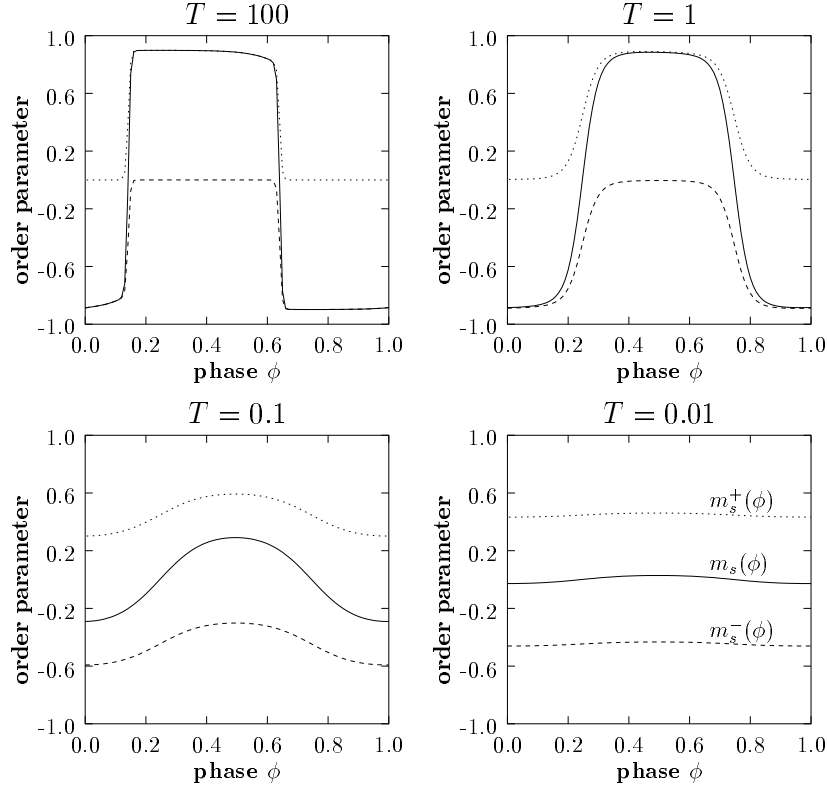


Figure 4: Order parameters $m_s(t)$, $m_s^+(t)$, $m_s^-(t)$ as a function of the oscillation phase $\phi = (t \bmod T)/T$ in a landscape with two alternating peaks. The upper dashed line represents $m_s^+(t)$, the lower dashed line represents $m_s^-(t)$, and the solid line represents $m_s(t)$. The sequence length is $l = 10$, and we have used $R = 0.05$ and $n = T/\Delta t = 100$ in all four examples. The parameters of the fitness landscape are $A_{0,\text{stat}} = e^{2.4}$, $\epsilon = 2$.

which is a degenerate landscape with two peaks of equal height. As noted above, the quasispecies becomes symmetric in such a landscape. In the lower right plot of Fig. 4, for $T = 0.01$, we can identify this limiting behavior. Both $m_s^+(t)$ and $m_s^-(t)$ are nearly constant over the whole oscillation period with an absolute value close to 0.5. The deviation from 0.5 stems from the finite value of the error rate, $R = 0.05$ in this example. We observe further that $m_s(t)$ lies very close to zero, thus wrongly indicating a disordered state. Note that the absolute value of $m_s^\pm(t)$ for a uniformly spread population lies for the parameters of this example at 0.12 according to Eq. (69).

The observations from the landscape with two oscillating peaks have to be interpreted in the light of the results of Schuster and Swetina on static landscapes

with two peaks [28]. They have found that if the peaks are far away in Hamming distance (which is the case here), a quasispecies is generally unable to occupy both peaks at the same time, unless they are of exactly the same height and with the same neighborhood.¹ For two peaks with different heights, the quasispecies will for small R generally form around the higher peak. For larger R , however, the quasispecies moves to the lower peak if this one has a higher mutational backflow from mutants, which is the case, for example, if the second peak is broader than the first one. The transition from the higher peak to the lower one with increasing R is very sharp, and can be considered as a phase transition. In a dynamic landscape with relatively slow changes, the quasispecies therefore switches the peak quickly when the higher peak becomes the lower one and vice versa.

The exact time at which the switch occurs depends of course on the error rate. The lower the error rate, the longer does the population remain centered around the previously higher peak until it actually moves on to the new higher peak. Therefore, if we look at the system at a fixed phase, and change the error rate, the quasispecies does, for certain phases ϕ , undergo a transition similar to the one found in [28] for static landscapes. This is illustrated in Fig. 5, where we display the order parameter m_s as a function of the error rate R . At the beginning of the oscillation period, for $\phi = 0$, the quasispecies is, for all error rates R below the error threshold, dominated by the peak corresponding to $m_s = -1$. This must be the case, as the replication coefficients of the two peaks intersect at $\phi = 0$, so up to this point the quasispecies has not had a chance to build up around the other peak. For phases shortly after $\phi = 0$, the quasispecies gains weight around the other peak, starting from the error threshold on downwards. For $\phi = 0.15$, for example, we observe a relatively sharp transition from the peak corresponding to $m_s = -1$ to the peak corresponding to $m_s + 1$ at $R \approx 0.05$. The transition then moves quickly towards $R = 0$, until the peak corresponding to $m_s = 1$ dominates the quasispecies for all R . For $\phi = 0.5$, the replication coefficients intersect again, and the quasispecies is exactly the inverse of the one for $\phi = 0$.

3.3.3 Two oscillating peaks with flat average landscape

In Sec. 3.1.3, we have predicted a special phase diagram for landscapes whose time average is completely flat. A particular realization of such a landscape is obtained if all replication coefficients are either set to a constant a or to a function $a + b_i \sin(\omega t + \delta_i)$, with arbitrary δ_i and $b_i < a$. In comparison to the previous subsection, here we choose again a landscape in which a sequence and its inverse

¹This is only true for infinite populations, however. For finite populations, one of the two peaks will always get lost eventually due to sampling fluctuations.

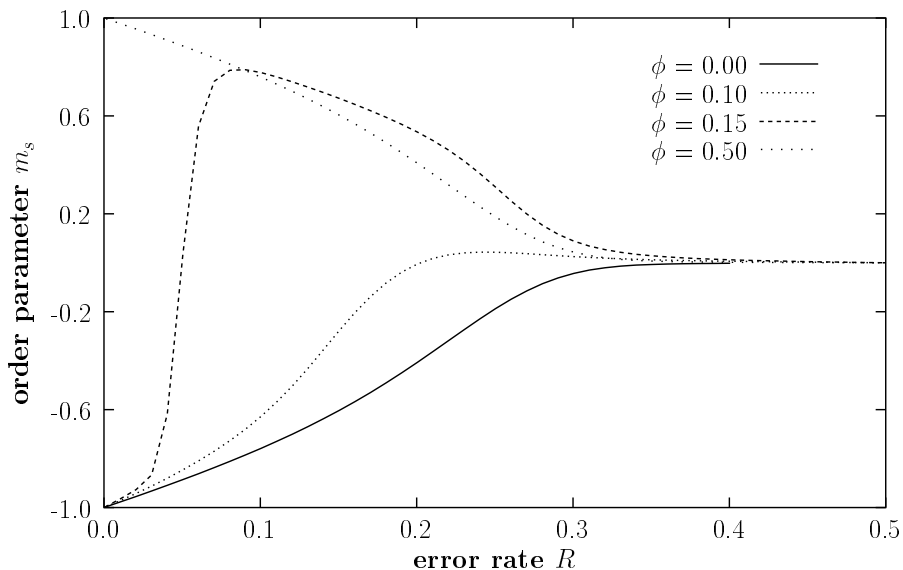


Figure 5: The order parameter m_s as a function of the error rate R for various oscillation phases $\phi = (t \bmod T)/T$. The fitness landscape is identical to the one of Fig. 4, and the oscillation period is $T = 100$. Note that for $\phi = 0.10$, the error threshold seems to have moved towards lower R , which is not the case. What we have instead is a symmetric population, as explained on page 22. A plot of m_s^+ or m_s^- reveals this immediately. However, we have not displayed such a plot here in order to enhance the clarity of this figure.

are alternating, while all others remain constant. We set the replication rates to

$$A_0(t) = 1 - b \sin \omega t, \quad (71a)$$

$$A_l(t) = 1 + b \sin \omega t, \quad (71b)$$

$$A_i(t) = 1 \quad \text{for } 0 < i < l. \quad (71c)$$

The order parameter of the quasispecies in such a landscape is displayed in Fig. 6 as a function of R for various oscillation periods T . What is immediately apparent from the plot is the existence of a lower error threshold in addition to the normal upper error threshold. This is in perfect agreement with the phase diagram in Fig. 2b), which predicts such a lower error threshold for landscapes with a flat average. With decreasing length T of the oscillation period, the two thresholds approximate each other, reducing the region in which order can be seen. For $T = 20$, the order parameter does not even reach the value $m_s = 0.1$ anymore, and for $T = 10$, it would be indistinguishable from the R -axis in this plot.

To be able to study the region of small T in more detail, we have done an expansion of \mathbf{X} in terms of T as given in Eq. (29), up to second order. The

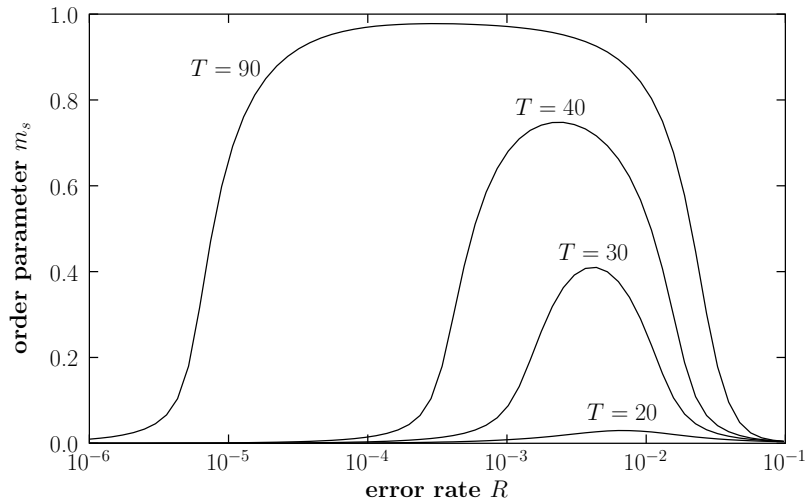


Figure 6: The order parameter m_s as a function of R in a landscape with two alternating peaks that average to a flat landscape [Eq. (71)]. In this case, $m_s = 0$ corresponds always to true disorder, and therefore, we have refrained from displaying m_s^+ and m_s^- in addition to m_s , in order to enhance the clarity of the plot. The other parameters were $l = 10$, $b = 9/10$, $\phi = 0$ and $n = T/\Delta t = 100$.

corresponding integrals can be taken relatively easy for this particular landscape. The details of the calculation are given in Appendix A. By comparing the results from this expansion with the results from the discrete approximation Eq. (52), this serves also as a test of the validity of Eq. (29).

In Fig. 7, we have displayed the order parameter m_s obtained from the expansion of \mathbf{X} in terms of T and from the discrete approximation of \mathbf{X} as a function of the phase ϕ for four different oscillation periods T .

First of all, the order parameter clearly flattens out for $T \rightarrow 0$ (note that the ordinates are scaled differently in the four plots, which may obfuscate this fact on first glance). However, since the T^2 term in the expansion gives a time-dependent contribution for arbitrarily small T [Eq. (128)], we cannot define the transition point to complete disorder with rigor. But this is nothing new. The same applies to the standard error threshold in a static landscape. Analytically, the order parameter never reaches zero for a finite string length l and for $R < 0.5$. This is related to the fact that the error transition is a surface transition with complete wetting [30]. Since the surface is finite, the order parameter indicating this surface transition remains always finite. Hence, the exact transition point can only be determined from the corresponding transition in the bulk. For our purposes here, it suffices to note that for a finite oscillation period, here about $T = 10$, the order

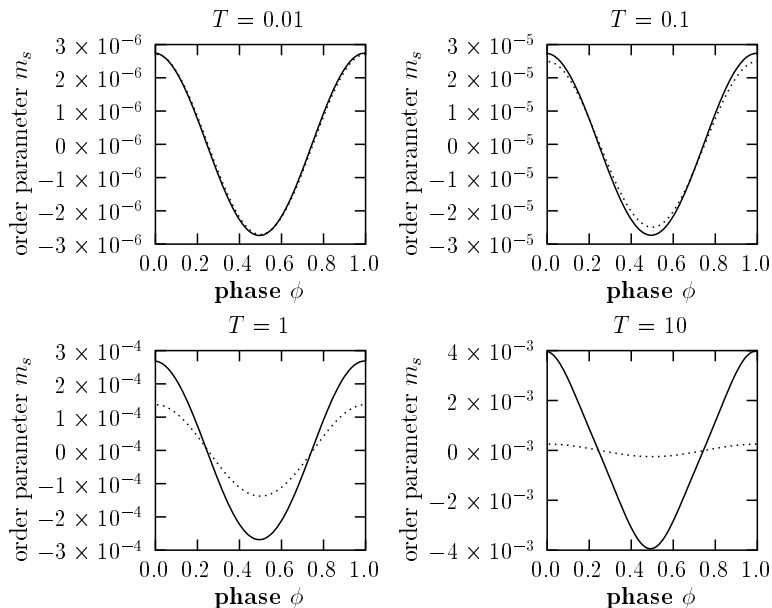


Figure 7: The order parameter m_s for a landscape in which a sequence and its inverse become alternatingly the master sequence. The error rate is $R = 0.01$. The solid lines give stem from the discrete approximation, the dotted lines stem from the expansion in terms of T , Eq. (29), evaluated up to second order. Clearly, the expansion Eq. (29) is only of use for relatively short oscillation periods.

parameter is almost zero for all replication rates R . This demonstrates that the phase diagram Fig. 2b) is indeed correct.

Second of all, we observe that the expansion in terms of T breaks down for T larger than ≈ 1 . This agrees well with our estimate for the radius of convergence of the expansion given in Eq. (40), which guarantees convergence only for $T < 1$ in the present case.

4 Aperiodic or stochastic fitness landscapes

Periodic fitness landscapes can be treated rather elegantly. We have been able to define a meaningful quasispecies, as well as we have been able to determine the general dynamics in the border regions of the parameter space. It would be desirable to obtain similar results for arbitrary dynamic landscapes. After all, an aperiodic or stochastic change is much more realistic than an exactly periodic change. However, the definition of a time-dependent quasispecies is tightly connected to periodic fitness landscapes. For arbitrary changes, it does not make sense

to speak of an asymptotic state. Regardless of that, we can derive some results for the border regions of the parameter space. In Section 3.1, we derived the formal solution to Eq. (6),

$$\mathbf{y}(t_0 + \tau) = \sum_{k=0}^{\infty} \tau^k \overline{\mathbf{W}}_k(t_0, \tau) \mathbf{y}(t_0). \quad (72)$$

To first order in τ , the formal solution reads

$$\mathbf{y}(t_0 + \tau) = \mathbf{y}(t_0) + \tau \overline{\mathbf{W}}_1(t_0, \tau) \mathbf{y}(t_0). \quad (73)$$

Obviously, the composition of the sequence distribution changes very little over the interval $[t_0, t_0 + \tau]$ if the condition

$$\tau \|\overline{\mathbf{W}}_1(t_0, \tau)\|_1 \ll 1 \quad (74)$$

is satisfied. This observation allows us to establish a general result for quickly changing fitness landscapes. If the landscape changes in such a way that for every interval of length τ beginning at time t_0 , the average

$$\overline{\mathbf{W}}_1(t_0, \tau) = \frac{1}{\tau} \int_0^\tau \mathbf{W}(t_0 + \tau_1) d\tau_1 \quad (75)$$

is approximately the same for every t_0 , and the condition $\|\overline{\mathbf{W}}_1(t_0, \tau)\| \ll 1/\tau$ holds, then the system develops a quasispecies given by the normalized principal eigenvector of the average matrix $\overline{\mathbf{W}}_1(t_0, \tau)$. With “approximately the same” we mean that for two times t_0 and t_1 , the components of the averaged matrices satisfy

$$\left| \left(\overline{\mathbf{W}}_1(t_0, \tau) \right)_{ij} - \left(\overline{\mathbf{W}}_1(t_1, \tau) \right)_{ij} \right| < \epsilon \quad \text{for all } i, j, t_0, t_1, \quad (76)$$

with a suitably small ϵ . In other words, if the fitness landscape changes very fast, but in stationary way, then the evolving population sees only the time-averaged fitness landscape.

For the special case of $R = 0$, we can, as in Eq. (43), write the solution for the quasispecies equation as

$$\mathbf{y}(t) = \exp \left(\int_{t_0}^t [\mathbf{A}(t') - \mathbf{D}(t')] dt' \right) \mathbf{y}(t_0). \quad (77)$$

Unlike in the case of a periodic landscape, however, this does not tell us the general behavior at $R = 0$, apart from the fact that for fast changes, the system sees the average fitness landscape. But we knew that already from Eq. (73). If we have the

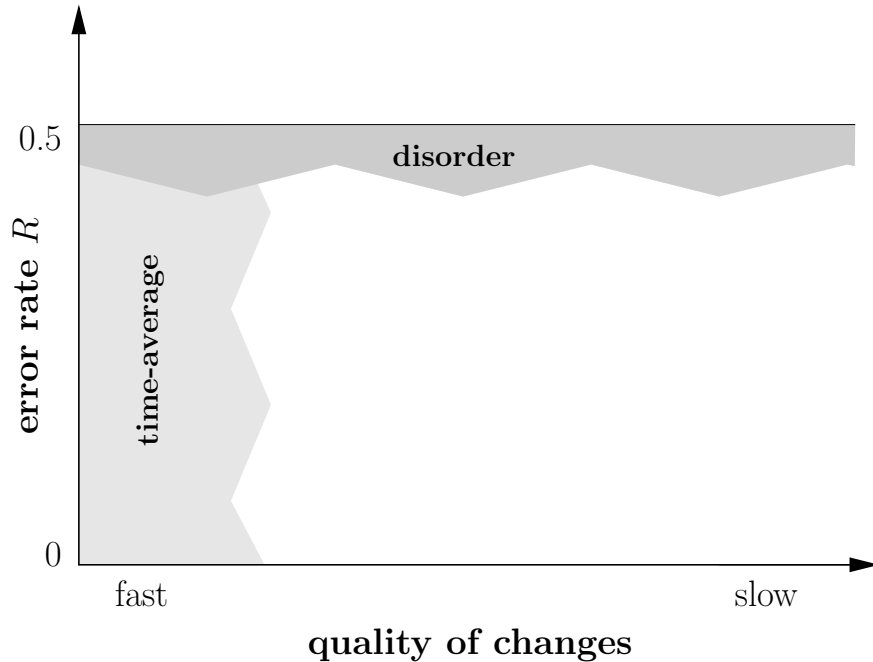


Figure 8: The appearance of a stochastic fitness landscape at the border regions of the parameter space.

situation of a stochastic landscape with long time correlations, on the other hand, it is hard to make general statements. The reason for this is that from long time correlations, we cannot generally deduce that the system must be in a quasistatic state. It may be the case if, for example, the landscape changes only rarely, but then drastically. On the other hand, one can easily come up with landscapes that are in a constant flux, and still display long time correlations. Hence, there exists no direct equivalent to the large oscillation period case of periodic fitness landscapes for general stochastic landscapes. Nevertheless, we can draw a diagram similar to Fig. 1, where on the x -axis we use the qualitative description “slow” and “fast” changes. Under “fast”, we subsume everything that satisfies the above stated conditions under which the system sees the average fitness landscape, and under “slow” we subsume everything else, assuming that a parameter exists that allows a smooth transition from the “fast” regime to the “slow” regime. Then, the analogue to Fig. 1 is Fig. 8. Although this figure contains considerably less information than Fig. 1, the implications for actual landscapes are more or less the same. Most real landscapes will have a regime that can be associated with slow changes, and hence, we will typically observe phase diagrams of the type of either Fig. 2a) or b).

As an example, consider the work of Nilsson and Snoad [19], and its subsequent extension by Ronnewinkel *et al.* [22]. Nilsson and Snoad have studied a landscape in which a single peak performs a random walk through the sequence space. The peak jumps to a random neighboring position of hamming distance 1 whenever a time interval of length τ has elapsed. Ronnewinkel *et al.* have studied a very similar fitness landscape, but they have mainly been interested in deterministic movements of the peak that allow for the formal definition of a quasispecies, similarly to the situation of periodic fitness landscapes in Section 3.1. Ronnewinkel *et al.* could verify the results of Nilsson and Snoad on more fundamental theoretical grounds.

The parameter τ in the jumping peak landscape determines whether the changes happen on a short or on a long time scale. If τ is very large, the landscape is static most of the time, and the population has enough time to settle into equilibrium before the peak jumps to a new position. If τ is very small, on the other hand, the peak has moved away long before the population has had the time to form a stable quasispecies. Nilsson and Snoad have found that, in addition to the common error threshold at which the mutation rate becomes too high to allow for quasispecies formation, another error threshold can be found at which the mutation rate becomes too low to allow the population to adapt to the changing landscape. The region of the lower disordered phase grows with decreasing τ , until the lower and the higher error threshold coincide and no selection can take place anymore. This is clear from an intuitive point of view. The faster the peak moves, the higher must the error rate be in order to allow the population to track the peak. Once the error rate needed to track the peak exceeds the highest error rate for which selection is possible, everything breaks down and the population does not feel any selective pressure any more. Nilsson and Snoad concluded therefore that “dynamic landscapes have strong constraints on evolvability”. However, this conclusion is not so straightforward if we reconsider their landscape from the viewpoint of the general theory developed here. As we have pointed out several times so far, the authoritative fitness landscape in the region of fast changes is the time averaged landscape. Thus, selection does not break down because of a fast changing landscape itself, but it breaks down due to the neutrality of the time-averaged landscape in this particular case. If there was a region in the sequence space in which the peak would assume a higher level than in the remaining sequence space, or if the peak’s movements were confined to a small portion of the sequence space, we would clearly see selection in these particular regions. This suggests the viewpoint that the time-averaged landscape gives the “regions of robustness” in the landscape, the regions in which even fast changes in the landscape do not destroy the quasispecies.

5 Finite Populations

In the previous sections, we have been studying infinite populations exclusively. However, the huge genotype spaces that are generated even by moderately long sequences (there are already 10^{30} different sequences of length 100, for example), will be almost empty for any realistic finite population. When most of the possible sequences are not present in the population, the concentration variables become useless, and the outcome of the differential equation formalism may be completely different from the actual behavior of the population. For static fitness landscapes, the effects of a finite population size are reasonably well understood. If the fitness landscape is very simple (a single peak landscape), the population is reasonably well described by finite stochastic sampling from the infinite population concentrations. Moreover, the error threshold generally moves towards smaller R with decreasing population size [20]. In a multi peak landscape, the finite population localizes relatively fast around one peak, and there it remains, with a dynamics similar to that in a single peak landscape. In the rare case that a mutant discovers a higher peak, the population moves over to that peak, where it remains again. The main difference between a finite and an infinite population on a landscape with many peaks is given by the fact that the infinite population will always build a quasispecies around the highest peak, whereas the finite population may get stuck on a suboptimal peak. Above the error threshold, a finite population starts to drift through the genotype space, irrespective of the landscape.

A finite population on a dynamic landscape will of course show a similar behavior, but in addition to that, other effects come into play that are tightly connected to the dynamics of the landscape. The most important difference between static and dynamic landscapes is the possible existence of a temporarily ordered phase in the latter case, and there we should expect the major new dynamic effects.

In the infinite population limit, the temporarily ordered phase generates an alternating pattern of a fully developed quasispecies and a homogeneous sequence distribution. What changes if a finite population evolves in that phase? At those points in time when a quasispecies is developed, the finite population's sequence concentrations are given by stochastic sampling from the infinite population result, similarly to static landscapes. As soon as the quasispecies breaks down (and this may happen earlier than the infinite population equations predict, because of the error threshold's shift to a lower error rate for a finite population), the population starts to disperse over the landscape. Because of that, the population may lose track of the peak it was centered about previously. Therefore, when it enters again a time interval in which order should be seen, the population may not be able to form a quasispecies, thus effectively staying in the disordered regime, or it may form a quasispecies at a different peak. In that way, the temporarily ordered phase

can open up a third possibility for a population to leave a local peak, in addition to the escape via neutral paths or to entropy-barrier crossing, which are present exclusively in static landscapes [32].

5.1 Numerical results

The numerical results presented below have been obtained from a genetic algorithm with N sequences per generation. We have used the following mutation and selection scheme in order to stay as closely as possible with the Eigen model:

1. To all sequences i in time step t , we assign a probability to be selected and mutated,

$$p_{i,\text{mutate}}(t) = \frac{A_i(t)}{\sum_i [1/\Delta t + A_i(t) - D_i(t)] n_i(t)}, \quad (78)$$

and a probability to be selected but not mutated,

$$p_{i,\text{select}}(t) = \frac{1/\Delta t - D_i(t)}{\sum_i [1/\Delta t + A_i(t) - D_i(t)] n_i(t)}. \quad (79)$$

Here, Δt is the length of one time step, and $n_i(t)$ is the number of sequences of type i .

2. From the set of probabilities $\{p_{i,\text{mutate}}(t), p_{i,\text{select}}(t)\}$, we choose N sequences at random. These N sequences are going to form the population in time step $t + \Delta t$. A sequence j that is determined to be mutated is subsequently converted into sequence i according to the mutation matrix Q_{ij} .

Note that we assume generally

$$D_i(t) < \frac{1}{\Delta t} \quad \text{for all } i, t, \quad (80)$$

so that $p_{i,\text{select}}(t)$ defined in Eq. (79) is always positive.

For an infinite population, the above described genetic algorithm evolves according to the equation

$$\mathbf{x}(t + \Delta t) = G(\mathbf{x}(t), t), \quad (81)$$

where $\mathbf{x}(t)$ is the vector of concentrations at time t , and $G(\mathbf{x}, t)$ is the operator that maps a population at time t onto a population at time $t + 1$,

$$G(\mathbf{x}, t) = \frac{[\Delta t \mathbf{W}(t) + \mathbf{1}] \mathbf{x}}{e^t \cdot ([\Delta t \mathbf{A}(t) - \Delta t \mathbf{D}(t) + \mathbf{1}] \mathbf{x})}. \quad (82)$$

Since we can replace the non-linear operator $G(\mathbf{x}, t)$ with a linear operator $\tilde{G}(\mathbf{y}, t)$,

$$\tilde{G}(\mathbf{y}, t) = [\Delta t \mathbf{W}(t) + \mathbf{1}] \mathbf{y}, \quad (83)$$

in Eq. (81), if we recover the true concentrations \mathbf{x} via

$$\mathbf{x}(t) = \frac{\mathbf{y}(t)}{\mathbf{e}^t \cdot \mathbf{y}(t)}, \quad (84)$$

we have a direct correspondence between the genetic algorithm for an infinite population and the discrete quasispecies model, as can be seen by comparing Eq. (83) with Eq. (49). This implies in particular that for periodic landscapes, the expression for the monodromy matrix $\mathbf{X}(t_0)$, Eq. (52), is exact. There is no approximation involved.

For a finite population, it is still the operator $G(\mathbf{x}, t)$ that determines the dynamics. However, the deterministic description Eq. (81) has to be replaced by a probabilistic one, namely Wright-Fisher or multinomial sampling. If $G_i(\mathbf{x}, t)$ denotes the i th component of the concentration vector in the next time step, the probability that a population $\mathbf{x}_1 = (m_1, m_2, \dots)/N$, $\sum_i m_i = N$, produces a population $\mathbf{x}_2 = (n_1, n_2, \dots)/N$, $\sum_i n_i = N$, in the next time step, is given by

$$P(\mathbf{x}_1 \rightarrow \mathbf{x}_2, t) = N! \prod_i \frac{G_i(\mathbf{x}_1, t)^{n_i}}{n_i!}. \quad (85)$$

A proof that the stochastic process described by Eq. (85) does indeed converge to the deterministic process Eq. (81) in the limit $N \rightarrow \infty$ has been given by van Nimwegen *et al.* [33].

5.1.1 Loss of the master sequence

Our first example of a finite population in a dynamic fitness landscape demonstrates what happens if in the temporarily ordered phase the master sequence is lost due to sampling fluctuations. In Fig. 9, we have presented a run of a finite population consisting of $N = 1000$ sequences of length $l = 15$, initialized randomly at $t = 0$, in an oscillating Swetina-Schuster landscape. For a comparison, we have also plotted the theoretical result for an infinite population. The infinite population is always in an ordered state, the order parameter m_s never takes on values smaller than 0.2. Nevertheless, the finite population is likely to lose the master sequence whenever the order parameter of the infinite population reaches its minimum, since the error threshold is shifted towards lower error rates for finite populations. In our example run, the master sequence was lost at the end of

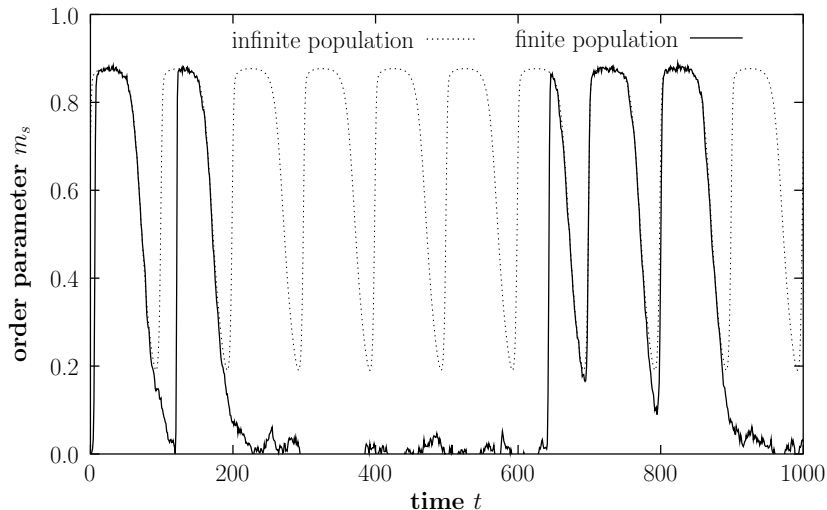


Figure 9: A single run of a population of $N = 1000$ sequences in the oscillating Swetina-Schuster landscape. The sequences had length $l = 15$. The other parameters were $A_0(t) = e^{2.4} \exp(2 \sin \omega t)$, $A_i = 1$ for $i > 0$, $R = 0.06$, $T = 100$, $\Delta t = 1$. The dashed line indicates the theoretical result for an infinite population.

the first oscillation period, but it was rediscovered shortly afterwards, so that the population could follow the infinite population dynamics for most of the second oscillation period as well. Right after a loss of the master sequence, the probability to rediscover the master has its highest value, because the population is still centered around the master sequence. Once the population has had the time to drift away from the position of the master sequence, the probability of a rediscovery drops rapidly. This is what happened at the end of the second oscillation period. The population completely lost track of the master sequence, and it took the population more than 4 oscillation periods to rediscover it. This is the main difference between a finite and an infinite population in the temporarily ordered phase. For an infinite population, the interval of disorder has the same well defined length in each oscillation period, whereas for a finite population, once the population has entered the disordered state, it may take a long time until an ordered state is reached again. In fact, for the case of a single peak in a very large sequence space and a small population, the peak may effectively be lost forever once it has disappeared from the population.

This can be seen as a dynamic version of Muller's ratchet [18]. A trait whose advantageous influence on the overall fitness of an individual is reduced at some point (it is not necessary that the trait becomes completely neutral or even deleterious) may get lost from the population due to sampling fluctuations. If then at

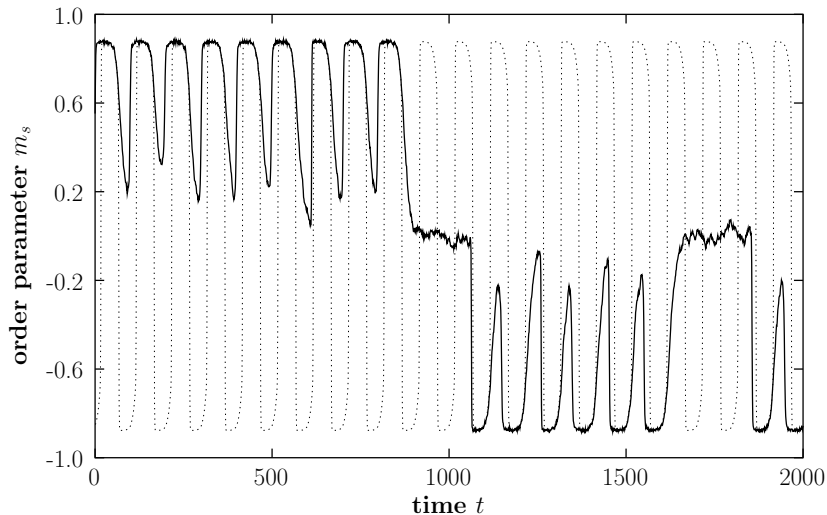


Figure 10: A single run of a population of $N = 1000$ sequences in a landscape as given in Eq. (64). All parameters were identical to the setup of Fig. 9. The dashed line again indicates the theoretical result for an infinite population.

a later stage this trait becomes again very advantageous, it is not available to the population anymore, until it is rediscovered independently. However, a rediscovery may be very unlikely.

5.1.2 Persistency

A second aspect of a finite population in a dynamic landscape is persistency. This means, a finite population may not be able to follow the changes in the landscape, although the infinite population limit predicts this. An example of that effect is given in Fig. 10. There, we have two alternating peaks at opposite corners of the boolean hypercube, as given by Eq. (64). Note that the peaks' minimal height is relatively small, but still larger than the rest of the landscape's height. In fact, all parameters are identical to the situation shown in Fig. 9, so that this figure can be seen as an example of the dynamics around one of the peaks in Fig. 10. The infinite population result in Fig. 10 predicts that the population should move on to the other peak whenever this peak becomes the higher one. However, the finite population does not follow this scheme. It stays localized around one of the two peaks for a long time. A finite population does not, unlike an infinite population, occupy all possible points in the sequence space at the same time. Therefore, if a peak grows at a distance too far from the currently occupied peak, no sequence in the population is there to exploit the advantage, and hence the new opportunity

goes undetected. Only if the population loses track of the first peak, which is possible because of the temporarily ordered phase, it can discover the second peak during its random drift. In the run of Fig. 10, this has happened two times. The first time, the population had discovered the alternative peak at the end of the drift, and the second time, it had again rediscovered this same peak.

The situation of a finite population in a dynamic landscape with several growing and shrinking peaks can be compared to its situation in a rugged, but static landscape. In the latter case, once the population has reached a local optimum it remains there, unless a rare mutation opens the possibility to move to a new, higher peak. The same applies to the dynamic situation. But in addition, the fluctuations and oscillations of the fitness values destabilize the population on local optima, and allow it to continue its search for other local optima. If the landscape’s dynamics is such that the population, by following the local optima, moves into regions of low average fitness (observed e.g. in [35]), the landscape might be called “deceptive”, and in the opposite case, it might be called “well-behaved”.

5.2 A finite population on a simple periodic fitness landscape

In the above examples, we saw that the time it takes until the master is rediscovered, once it has been lost in the temporarily ordered phase, may be much larger than the period length of the landscape. Hence, for several periods, the population does not follow the infinite population results, but remains in a disordered state. It would be desirable to have an analytic description of this behavior, and, in particular, to have an estimate of the probability with which a complete period is skipped, i.e., with which the master sequence is missed for a whole oscillation period. Unfortunately, the continuous time dependency of the master sequence’s replication rate employed in Sec. 5.1,

$$A_0(t) = A_{0,\text{stat}} \exp(\epsilon \sin \omega t), \quad (86)$$

renders the corresponding calculations very complicated. Therefore, in order not to get too distracted by technical details in the calculation, we study in this section a simplified fitness landscape that displays a temporarily ordered phase similar to Fig. 9, but that is much easier to handle analytically. For a fitness landscape such as Eq. (86), we can—for sufficiently high error rate R —divide the oscillation period into two intervals. During the first interval I_1 , of length T_1 , the population is in an ordered state provided that the master sequence is present in the population, and during the second interval I_2 , of length T_2 , the population is in a disordered state, even if the master sequence is present. The beginning of the first interval

need not coincide with the beginning of the oscillation period, but after a suitable shift of the time origin, this is always the case. Note that for a finite population, the second interval is larger than predicted by the infinite population limit, and it may exist even if the infinite population limit predicts a length $T_2 = 0$, because the error threshold is shifted towards smaller error rates for finite populations [20, 34]. This can be seen clearly in Fig. 9, where the infinite population limit predicts $T_2 = 0$, but the master is lost anyway because of sampling fluctuations.

Our approximation here is to keep the fitness landscape constant during the intervals I_1 and I_2 . During the interval I_1 , we let the master replicate with rate $A_0 \gg 1$, while all other sequences replicate with $A = 1$. During the second interval on the other hand, the fitness landscape becomes flat. Then, all sequences replicate with $A = 1$. We continue to study the discrete process and set $\Delta t = 1$, so that T_1 and T_2 give the number of time steps spent in each interval. In summary, the replication rate $A_0(t)$ satisfies

$$A_0(t) = \begin{cases} a: & \phi \leq T_1 \\ 1: & \text{else.} \end{cases} \quad (87)$$

In order to get expressions that can be easily treated even for a finite population, we use the error tail approximation introduced in [20]. In that approximation, the state of the system is fully described by the concentration of the master sequence. All other sequences are assumed to be uniformly spread over the remaining genotype space. This approximation underestimates the mutational backflow into the master sequence, and hence it underestimates the concentration of the master itself, but this small deviation can be accepted in the light of the enormous simplifications in the calculations.

Before we have a look at the finite population dynamics, let us quickly study the infinite population limit. We express the state of the system at time t by a vector $\mathbf{x}(t) = (x_0(t), x_1(t))^t$, where $x_0(t)$ gives the concentration of the master sequence, and $x_1(t) = 1 - x_0(t)$ gives the total concentration of all other sequences. The generation operator $G(\mathbf{x}, t)$ maps the population at time t into the population at time $t + 1$, i.e.,

$$\mathbf{x}(t + 1) = G(\mathbf{x}(t), t). \quad (88)$$

Here, $G(\mathbf{x}, t)$ is given by

$$G(\mathbf{x}, t) = \frac{[\mathbf{Q}A(t) + \mathbf{1}]\mathbf{x}}{A_0(t)x_0 + x_1 + 1}. \quad (89)$$

\mathbf{Q} is the 2×2 matrix

$$\mathbf{Q} = \begin{pmatrix} (1 - R)^l & \frac{1 - (1 - R)^l}{2^l - 1} \\ 1 - (1 - R)^l & 1 - \frac{1 - (1 - R)^l}{2^l - 1} \end{pmatrix}, \quad (90)$$

and $\mathbf{A}(t) = \text{diag}(A_0(t), 1)$. The linear operator $\tilde{\mathbf{G}}(t) = \mathbf{Q}\mathbf{A}(t) + \mathbf{1}$ describes the evolution of the variables $\mathbf{y}(t)$,

$$\mathbf{y}(t+1) = \tilde{\mathbf{G}}(t)\mathbf{y}(t), \quad (91)$$

which map into the original variables via

$$\mathbf{x}(t) = \frac{\mathbf{y}(t)}{\mathbf{e}^t \cdot \mathbf{y}(t)}, \quad \mathbf{e}^t = (1, 1). \quad (92)$$

Hence, the eigensystem of $\tilde{\mathbf{G}}$ fully describes the time evolution of $\mathbf{x}(t)$. For the eigenvalues of $\tilde{\mathbf{G}}$, we find

$$\lambda_{0,1} = \frac{1}{2} \left[\tilde{G}_{00} + \tilde{G}_{11} \pm \sqrt{(\tilde{G}_{00} - \tilde{G}_{11})^2 + 4\tilde{G}_{01}\tilde{G}_{10}} \right], \quad (93)$$

where the plus sign corresponds to the index 0, and the minus sign corresponds to the index 1. The eigenvectors are

$$\boldsymbol{\phi}_{0,1} = \frac{1}{1 + \xi_{\pm}} (1, \xi_{\pm})^t, \quad (94)$$

$$\text{with } \xi_{\pm} = \frac{\tilde{G}_{00} - \tilde{G}_{11}}{2\tilde{G}_{01}} \pm \frac{1}{\tilde{G}_{01}} \sqrt{\frac{1}{4}(\tilde{G}_{00} - \tilde{G}_{11})^2 + \tilde{G}_{01}\tilde{G}_{10}}. \quad (95)$$

Of course, the eigenvalues and the eigenvectors are different for the two intervals I_1 and I_2 . For the first interval, inserting the explicit expressions of \tilde{G}_{ij} into Eqs. (93)–(95) does not lead to a substantial simplification of the expressions, so we leave this out here. For the second interval, however, we find for the eigenvalues

$$\lambda_0^{(2)} = 2, \quad (96a)$$

$$\lambda_1^{(2)} = 2 - \frac{1 - (1 - R)^l}{1 - 2^{-l}}, \quad (96b)$$

and for the eigenvectors

$$\boldsymbol{\phi}_0^{(2)} = (2^{-l}, 1 - 2^{-l})^t, \quad (97a)$$

$$\boldsymbol{\phi}_1^{(2)} = (1, -1)^t. \quad (97b)$$

The superscript (2) indicates that these results are only valid for the interval I_2 . From the above expressions, we get a simple formula for the evolution of the master's concentration during the interval I_2 . Let the interval start at time t , and

let the concentration of the master at that moment in time be $x_0(t)$. Then we find n time steps later

$$x_0(t+n) = \frac{\alpha_0 \phi_0^{(2)} + \alpha_1 \left(\lambda_1^{(2)} / \lambda_0^{(2)} \right)^n \phi_1^{(2)}}{\alpha_0 (\mathbf{e}^t \cdot \phi_0^{(2)}) + \alpha_1 \left(\lambda_1^{(2)} / \lambda_0^{(2)} \right)^n (\mathbf{e}^t \cdot \phi_1^{(2)})}, \quad (98)$$

where α_0 and α_1 have to be chosen such that

$$x_0(t) = \alpha_0 \phi_0^{(2)} + \alpha_1 \phi_1^{(2)}. \quad (99)$$

After solving Eq. (99) for α_0 and α_1 and inserting everything back into Eq. (98), we end up with

$$x_0(t+n) = 2^{-l} + [x_0(t) - 2^{-l}] \left(1 - \frac{1 - (1-R)^l}{2(1-2^{-l})} \right)^n. \quad (100)$$

This formula is sufficiently close to the solution obtained from diagonalization of the full $2^l \times 2^l$ matrix \mathbf{Q} in a flat landscape, and can be considered a good approximation to the actual infinite population dynamics [21]. In principle, a similar formula can be derived for the interval I_1 , but again, the expressions become very complicated, and do not lead to any new insight, so we leave this out here.

Equation (100) demonstrates that a macroscopic proportion of the master sequence that may have built up during the interval I_1 quickly decays to the expected concentration in a flat landscape, 2^{-l} .

Now we address finite populations. We assume the duration of the interval I_1 is long enough so that the quasispecies can form. The asymptotic concentration of the master sequence can then be calculated from a birth and death process as done in [20]. The alternative diffusion approximation used in [34] is of no use here because it allows only replication rates A_0 of the form $A_0 = 1 + \epsilon$ with a small ϵ [11]. In [20], the probabilities p_k to find the master sequence k times in the asymptotic distribution are given by

$$p_k = \frac{\tilde{p}_k}{\sum_{i=0}^N \tilde{p}_i} \quad \text{with } \tilde{p}_k = \frac{\mu_{k-1}^+}{\mu_k^-} \tilde{p}_{k-1} \text{ and } \tilde{p}_0 = 1. \quad (101)$$

The probabilities μ_i^+ and μ_i^- read here

$$\mu_i^+ = \frac{N-i}{N} \left(\left[\tilde{G}_{00}^{(1)} - 1 \right] \frac{i}{N} + \tilde{G}_{01}^{(1)} \frac{N-i}{N} \right) \quad (102)$$

and

$$\mu_i^- = \frac{i}{N} \left(\tilde{G}_{10}^{(1)} \frac{i}{N} + \left[\tilde{G}_{11}^{(1)} - 1 \right] \frac{N-i}{N} \right). \quad (103)$$

The expected asymptotic concentration becomes

$$x_0(\infty) = \frac{1}{N} \sum_{k=0}^N k p_k. \quad (104)$$

Unfortunately, there exists no analytic expression for $x_0(\infty)$. However, its value is easily computed numerically. By our above assumption on the length of the interval I_1 , we can suppose that at the end of I_1 , the concentration of x_0 is given by $x_0(\infty)$. During the interval I_2 , the concentration of the master will then decay.

5.2.1 The probability to skip one period

If at the end of the interval I_2 the master sequence has been lost because of sampling fluctuations, and if in addition to that the correlations in the population have decayed so far that we can assume maximum entropy, what is the probability that the master sequence is rediscovered in the following interval I_1 ? The process of rediscovering the master consists of two steps. The master sequence has to be generated through mutation, and then it has to be fixated in the population, i.e., it must not get lost again due to sampling fluctuations. First of all, we calculate the probability P_{miss} that the master is not generated in one time step. This corresponds to the probability that the multinomial sampling of the operator $G^{(1)}(\mathbf{x})$ maps a population $\mathbf{x} = (0, 1)^t$ into itself. Hence, we have

$$\begin{aligned} P_{\text{miss}} &= N! \prod_{i=0}^1 \frac{G_i^{(1)}(\mathbf{x})^{n_i}}{n_i!} \\ &= \left(\frac{Q_{11} + 1}{2} \right)^N = \left[1 - \frac{1 - (1 - R)^l}{2^{l+1} - 2} \right]^N. \end{aligned} \quad (105)$$

$G_i^{(1)}(\mathbf{x})$ stands for the i th component of the outcome of $G^{(1)}(\mathbf{x})$.

The probability that the master sequence gets fixated needs more work. Let $\pi(x, t)$ denote the probability that the master sequence has reached its asymptotic concentration at time t , given that it had the initial concentration x at time $t = 0$. The asymptotic concentration is given by $x_0(\infty)$ defined in Eq. (104). Then, the probability $\pi(x, t)$ satisfies to second order the backward Fokker-Planck equation

$$\frac{\partial \pi(x, t)}{\partial t} = \langle dx_0 \rangle \frac{\partial \pi(x, t)}{\partial x} + \frac{\langle (dx_0)^2 \rangle}{2} \frac{\partial^2 \pi(x, t)}{\partial x^2}. \quad (106)$$

The moments $\langle dx_0 \rangle$ and $\langle (dx_0)^2 \rangle$ can be calculated similarly to the calculations

in [33], and we find

$$\langle dx_0 \rangle = \left(\frac{1}{2} \lambda_0^{(1)} - 1 \right) x_0 =: \gamma x_0, \quad (107)$$

$$\langle (dx_0)^2 \rangle = \frac{x_0(1-x_0)}{N}. \quad (108)$$

The solution to Eq. (106) for $t \rightarrow \infty$ is then obtained as in [33], and we find

$$\pi_\infty := \pi \left(\frac{1}{N}, \infty \right) = \frac{1 - \left(1 - \frac{1}{N}\right)^{2N\gamma+1}}{1 - \left(1 - x_0(\infty)\right)^{2N\gamma+1}} \quad (109)$$

$$\approx 1 - e^{-2\gamma}. \quad (110)$$

As the initial concentration of x_0 , we have used $1/N$, since it is—for the parameter settings we are interested in—extremely unlikely that more than one master sequence is generated in one time step. The approximation in the second line is only valid for large population sizes. It generally underestimates the true value of π_∞ .

Note that the expression for π_∞ given in Eq. (109) reaches the value 1 for the (relatively large) error rate R close to the error threshold for which $x_0(\infty) = 1/N$. Naively, one would assume that π_∞ decays with increasing error rate, since mutations increase the risk that good traits are lost, and indeed the approximate expression in Eq. (110) decays with increasing error rate. However, since π_∞ is the probability that the master sequence reaches its equilibrium concentration, and the equilibrium concentration vanishes close to the error threshold, π_∞ must rise to 1 at the error threshold.

We have done some measurements with a finite population to test the validity of Eq. (109). For a number of runs, we have initialized the population at random, but with exactly one instance of the master sequence, and have counted how often the master's concentration reached $x_0(\infty)$ and how often it reached 0. The results of these measurements are shown in Fig. 11. Clearly, numerical and analytical results are in good agreement.

Finally, we need an estimate of the time τ it takes from the time step the master sequence is discovered to the time step in which the equilibrium concentration is reached for the first time. We follow again the calculations in [33], and assume that the process of fixation can be treated in the infinite population limit. From Eq. (89), we obtain for the change in the variable $x_0(t)$ during one time step in the interval I_1

$$x_0(t+1) - x_0(t) = \frac{-(a-1)x_0(t)^2 + (Q_{00}a - Q_{01} - 1)x_0(t) + Q_{01}}{(a-1)x_0(t) + 2}. \quad (111)$$

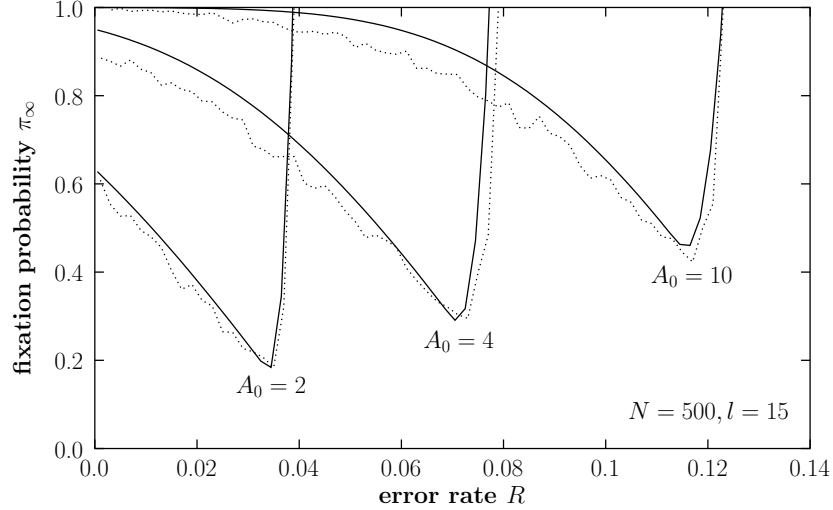


Figure 11: The fixation probability π_∞ as a function of the error rate R for three different heights of the peak. The solid lines stem from the analytic expression Eq. (109), and the dotted lines stem from measurements on a finite population consisting of $N = 500$ sequences.

We approximate this with a differential equation,

$$\frac{dx_0(t)}{dt} \approx x_0(t+1) - x_0(t), \quad (112)$$

which we can solve for t as a function of x_0 , and obtain

$$t = \frac{b+4}{z} \left(\text{Atanh} \frac{b-2sx_0}{z} - \text{Atanh} \frac{b-2s/N}{z} \right) - \frac{1}{2} \ln \frac{-sx_0^2 + bx_0 + Q_{01}}{-s/N^2 + b/N + Q_{01}}, \quad (113)$$

with

$$s = a - 1, \quad (114)$$

$$b = Q_{00}a - Q_{01} - 1, \quad (115)$$

and

$$z = \sqrt{4sQ_{01} + b^2}. \quad (116)$$

Therefore, for the estimated time it takes until the master sequence gets fixated we will use in the following

$$\tau = t(x_0(\infty)), \quad (117)$$

with $x_0(\infty)$ given in Eq. (104).

Hence, we can now calculate the probability that the population skips a whole period, i.e., that it does not find and fixate the master during one interval I_1 . The probability that the master sequence has concentration zero at the beginning of the interval I_1 is $(1 - 1/2^l)^N$. Therefore, the probability that the master sequence is not fixated in the first time step reads

$$1 - \left[1 - \left(1 - \frac{1}{2^l} \right)^N \right] \pi_\infty. \quad (118)$$

The probability that the master sequence does not get found and subsequently fixated in a subsequent time step is given by

$$1 - (1 - P_{\text{miss}}) \pi_\infty. \quad (119)$$

Now, if the master sequence is found, it will roughly take the time τ given in Eq. (117) until the equilibrium concentration is reached. Therefore, if the master sequence is not found during the first $T_1 - \tau$ time steps, it normally will not reach the equilibrium concentration anymore in that period. Therefore, in order to calculate the probability $P_{\text{skip}}(T_1)$ that the whole interval I_1 is skipped, we have to consider only the first $T_1 - \tau$ time steps of I_1 . In case that $T_1 < \tau$, we have $P_{\text{skip}}(T_1) \approx 1$. We have only approximate equality because τ is the average time until fixation occurs. In rare cases, the fixation may happen much faster.

Of the $T_1 - \tau$ time steps, the first one is different because in that time step we do not know whether the master sequence is present or not, whereas for the remaining $T_1 - \tau - 1$ time steps, we may assume that the master sequence is not present if fixation has not occurred. Therefore, we find

$$P_{\text{skip}}(T_1) = \left(1 - \left[1 - \left(1 - \frac{1}{2^l} \right)^N \right] \pi_\infty \right) [1 - (1 - P_{\text{miss}}) \pi_\infty]^{T_1 - \tau - 1} \quad (120)$$

$$\approx \frac{1 - \left[1 - \left(1 - \frac{1}{2^l} \right)^N \right] \pi_\infty}{1 - (1 - P_{\text{miss}}) \pi_\infty} \exp [-(T_1 - \tau) (1 - P_{\text{miss}}) \pi_\infty]. \quad (121)$$

Figure 12 shows a comparison between this result and numerical measurements. The measurements were taken by letting a randomly initialized population evolve in a flat landscape for 100 generations, and then recording the time it took the population to find and fixate a peak that was switched on in generation 101. We observe that the analytic expression for $P_{\text{skip}}(T_1)$ predicts the right order of magnitude and the right functional dependency on T_1 , but that it generally underestimates the exact value. Since Eq. (120) contains three quantities for which

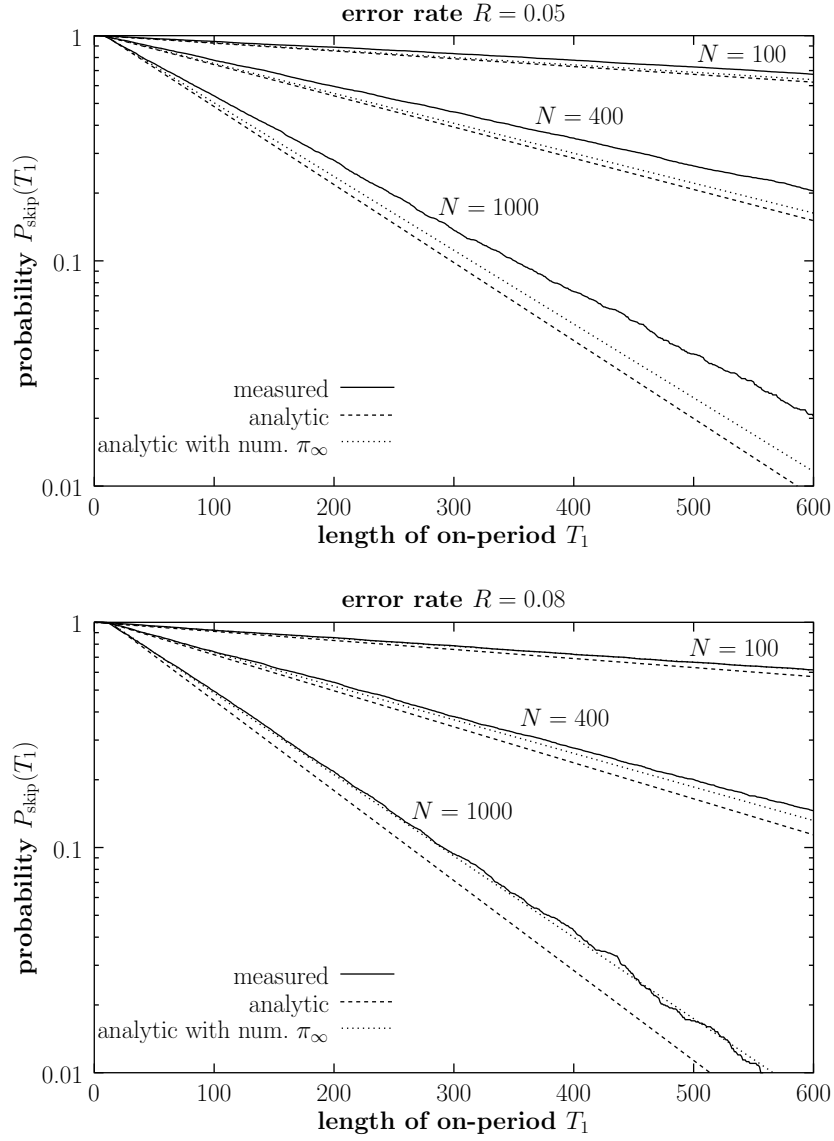


Figure 12: The probability $P_{\text{skip}}(T_1)$ that the population skips a whole period without fixating the master sequence, as a function of the length of the interval I_1 , for several different settings of N and R . The string length is $l = 15$.

we have only approximative expressions, namely P_{miss} , π_∞ , and τ , at first it is not clear from where these discrepancies arise. However, a systematic check quickly reveals the main cause of the discrepancies. First of all, note that τ merely shifts the curve to the right. Since the measured and the analytic curves reach the value 1 at very much the same positions in Fig. 12, we can assume that τ , as given by Eq. (117), is accurate enough for our purposes here. Now consider the quantity π_∞ . In Fig. 11, we saw that our expression for π_∞ generally gives a good estimate of the true value, but that there are some deviations. To check whether these deviations are responsible for the discrepancies visible in Fig. 12, we have additionally displayed $P_{\text{skip}}(T_1)$ with π_∞ determined from measurements. We find that the usage of the true value of π_∞ enhances the quality of Eq. (120), in particular for larger error rates. For small error rates, however, it does not help much. Moreover, the analytic expression is generally getting worse for smaller error rates. As a conclusion, the main problems arise from the expression for P_{miss} , Eq. (105). We have derived P_{miss} under a maximum entropy assumption, i.e., we have assumed that all mutants are distributed homogeneously over the sequence space. Under this assumption, the probability to find the master is exactly the same in every time step. But in reality, the population collapses very rapidly, even in a neutral landscape, and then moves about as a cluster whose radius is determined by the error rate. This introduces very long range time correlations in a population evolving in a flat landscape [5]. In particular for small error rates, the cluster is very small, and this can increase the probability P_{miss} substantially. Note that this effect corresponds to the underestimation of epoch durations that van Nimwegen *et al.* found in their analysis of the Royal Road genetic algorithm [33]. An exact treatment of this effect would probably have to be done along the lines of [5]. Unfortunately, we cannot simply use their expressions here, because of the term $+1$ present in our definition of the operator $G(\mathbf{x}, t)$ [Eq. (89)].

In order to check the hypothesis that the violation of the maximum entropy condition causes the main discrepancies shown in Fig. 12, we did some additional measurements in which we dispersed the population “by hand” over the complete sequence space except the master in every time step in which the master sequence was not discovered. With this setup, we found a very good agreement between the numerical and the analytical results.

Since it is the population’s collapse into a small cluster that causes the deviations between Eq. (120) and the measured $P_{\text{skip}}(T_1)$, it is clear that the true $P_{\text{skip}}(T_1)$ must always be larger than predicted by Eq. (120). Therefore, we can use that equation as a lower bound on the true value.

We notice that $P_{\text{skip}}(T_1)$ decays exponentially. This means that the probability

to find the peak in one oscillation period,

$$P_{\text{find}}(T_1) = 1 - P_{\text{skip}}(T_1), \quad (122)$$

approaches 1 for large T_1 . This is due to the fact that the peak will certainly be rediscovered if only we wait long enough. However, the model we are studying here is that of a peak that gets switched on and off alternatingly, and for which each “on”-period is of fixed length T_1 . In that case, the probability to rediscover the peak within one oscillation period can be extremely small, as we are going to see now. $P_{\text{skip}}(T_1)$ decays with a rate of $(1 - P_{\text{miss}})\pi_\infty$. We can neglect π_∞ here, as it is of the order of one. Then, the decay rate is for fixed N and large l approximately given by

$$1 - P_{\text{miss}} \approx N \frac{1 - (1 - R)^l}{2^{l+1}}, \quad (123)$$

i.e., it decays as 2^{-l} . This implies in turn that already for string lengths of 50–60 (which can be considered a rough lower bound for typical DNA sequence lengths) and moderate N and R , we have $P_{\text{find}}(T_1) \approx 0$ for moderate T_1 . Hence, in many cases it is extremely unlikely that the peak is rediscovered at all.

The above conclusion is of course tightly connected to the fact that we have studied a landscape with a single advantageous sequence. In the other extreme of a mount Fujiama landscape, in which the population can sense the peak from every position in the sequence space, the conclusions would look differently. Note, however, that neither the single sharp peak landscape nor the mount Fujiama landscape are realistic landscapes. In a realistic, high-dimensional rugged landscape, it is probably valid to assume that local optima, once they are lost from the population, are never rediscovered. In such situations, dynamic fitness landscapes can induce the loss of a local optimum, and thus, they can accelerate Muller’s ratchet[18] like effects.

6 Conclusions

In this paper, we have been able to derive several very general results on landscapes with periodic time dependency. First of all, a quasispecies can be defined by means of the monodromy matrix. This means that after a sufficiently long time, the state of the system depends only on the phase $\phi = (t \bmod T)/T$ of the oscillation, but it does not depend on the absolute time t any more. Therefore, in periodic fitness landscapes, the quasispecies is not a fixed mixture of sequence concentrations. Instead, it is a T -periodic function of mixtures of sequence concentrations. We

have given an expansion of the monodromy matrix in terms of the oscillation period T , which leads to an extremely simple description of the system for very high oscillation frequencies. Namely—if we assume the mutation matrix remains constant all the time—the time-averaged fitness landscape completely determines the behavior of the system; the system becomes indistinguishable from one in a static landscape. This leads to the important conclusion that selection never ceases to exist, no matter how fast the landscape changes. The only exception to this rule is generated by dynamic landscapes that have a completely flat average. In that case, the system behaves for very fast changes as being in a flat landscape, which is indistinguishable from the behavior of a system above the error threshold. Therefore, if the average landscape is flat, selection will break down if the changes occur with a frequency higher than some critical frequency $\omega^* = 2\pi/T^*$. For very slow changes, on the other hand, the system is virtually in equilibrium all the time. This leads generally to a time dependent error threshold $R^*(t)$. For mutation rates R such that $\min_t R^*(t) < R < \max_t R^*(t)$, the system is below the error threshold for some times t , and it is past the error threshold for other times. We have dubbed this region of the parameter space the temporarily ordered phase, as we see alternating patterns of order and disorder in that phase (in the infinite population limit). We found these general considerations to be in complete agreement with all example landscapes that we studied.

For the case of non-periodic landscapes, we have argued that the main conclusions remain valid, even if our mathematical formalism is not generally applicable in that case. Fast changes in the landscape will average out, whereas slow changes lead to a quasistatic adaption of the quasispecies to the current landscape. With these concepts, it has been possible to give an explanation for the occurrence of a lower error threshold in the work of Nilsson and Snoad [19].

While the molecular concentrations become T -periodic for $t \rightarrow \infty$ in the infinite population limit, this is not necessarily the case when we consider finite populations. In the temporarily ordered phase, after a population has made the transition to the disordered state, it is not said that it transitions back to order the same moment the infinite population would. Rather the opposite is the case. Once the population has lost the ordered state, it is often hard for it to return there. From a very simple analytical model, we have found that the probability that the ordered state is not rediscovered in one oscillation period decays exponentially in the length of the interval in which order is possible at all. The decay constant, however, is extremely small for large l , and therefore the rediscovery can become very unlikely. In more complex landscapes, this can lead to an acceleration of Muller’s ratchet.

Throughout this paper, we have assumed that mutations arise in the copy pro-

cess. An equally valid assumption is that of mutations arising on a per-unit-time basis (cosmic ray mutations), as opposed to the per generation basis implied by copy mutations. With the latter assumption, one has to study the parallel mutation and selection equations [3] instead of Eigen's equations. Since these equations can be linearized in the same way as the quasispecies equations, the formalism we developed applies also for these equations. The only difference between the two types of equations is that in the parallel case, the mutation matrix \mathbf{Q} and the replication matrix \mathbf{A} are added, whereas in the quasispecies case they are multiplied.

In future work, it should be tried to obtain an improved understanding of the properties of the monodromy matrix. In particular, an expansion of that matrix in the error rate R would certainly be valuable.

A High-frequency expansion of $\mathbf{X}(t)$ for a landscape with two alternating master sequences

With Eq. (29), we have given an expansion of the monodromy matrix for periodic landscapes, $\mathbf{X}(t_0)$, in terms of the period length T . Here, we want to calculate the expansion explicitly up to second order for an example landscape. In that landscape, there are two sequences (without loss of generalization, we assume them to be $i = 0$ and $i = 1$) that become alternately the master sequence. The replication rates are

$$A_0(t) = a + b \sin(\omega t), \quad (124a)$$

$$A_1(t) = c + d \sin(\omega t), \quad (124b)$$

$$A_i(t) = 1 \quad \text{for all } i > 1. \quad (124c)$$

The decay rates are set to zero. With vanishing decay rates, the matrix $\mathbf{W}(t)$ reduces to $\mathbf{QA}(t)$, and as a consequence, we can write the n th average $\overline{\mathbf{W}}_k(t)$ as

$$(\overline{\mathbf{W}}_k(t))_{ij} = \sum \nu_1 \sum \nu_2 \cdots \sum \nu_{k-1} Q_{i\nu_1} Q_{\nu_1\nu_2} \cdots Q_{\nu_{k-1}j} \overline{A}_{\nu_1, \nu_2, \dots, \nu_{k-1}, j}(t) \quad (125)$$

with the generalized replication coefficients

$$\begin{aligned} \overline{A}_{\nu_1, \nu_2, \dots, \nu_{k-1}, j}(t) &= \frac{1}{T^k} \int_0^T A_{i\nu_1}(t_0 + \tau_1) \int_0^{\tau_1} A_{\nu_2}(t_0 + \tau_2) \\ &\cdots \int_0^{\tau_{k-2}} A_{\nu_{k-1}}(t_0 + \tau_{k-1}) \int_0^{\tau_{k-1}} A_j(t_0 + \tau_k) d\tau_1 d\tau_2 \cdots d\tau_k. \end{aligned} \quad (126)$$

For the landscape given in Eq. (124), the first order tensor of the generalized replication coefficients has three independent elements, which are (assuming $i > 1$)

$$\bar{A}_0(t) = a, \quad (127a)$$

$$\bar{A}_1(t) = c, \quad (127b)$$

$$\bar{A}_i(t) = 1. \quad (127c)$$

The second order tensor has already 9 independent entries. After some algebra, we obtain (assuming again $i > 1$)

$$\bar{A}_{00}(t) = \frac{a^2}{2}, \quad (128a)$$

$$\bar{A}_{01}(t) = \frac{ac}{2} + \frac{ad - bc}{2\pi} \cos(\omega t), \quad (128b)$$

$$\bar{A}_{0i}(t) = \frac{a}{2} - \frac{b}{2\pi} \cos(\omega t), \quad (128c)$$

$$\bar{A}_{10}(t) = \frac{ac}{2} - \frac{ad - bc}{2\pi} \cos(\omega t), \quad (128d)$$

$$\bar{A}_{11}(t) = \frac{c^2}{2}, \quad (128e)$$

$$\bar{A}_{1i}(t) = \frac{c}{2} - \frac{d}{2\pi} \cos(\omega t), \quad (128f)$$

$$\bar{A}_{i0}(t) = \frac{a}{2} + \frac{b}{2\pi} \cos(\omega t), \quad (128g)$$

$$\bar{A}_{i1}(t) = \frac{c}{2} + \frac{d}{2\pi} \cos(\omega t), \quad (128h)$$

$$\bar{A}_{ii}(t) = \frac{1}{2}. \quad (128i)$$

In principle, the generalized replication coefficients $\bar{A}_{\nu_1, \nu_2, \dots, \nu_{k-1}, j}(t)$ can be calculated to arbitrary order for the landscape given in Eq. (124). However, the third order tensor has already 27 independent entries, and with every higher order, the number of independent entries triples.

References

- [1] Chris Adami and C. Titus Brown. Evolutionary learning in the 2D Artificial Life system 'Avida'. In Rodney A. Brooks and Pattie Maes, editors, *Artificial Life IV*, pages 372–381, Cambridge, MA, 1994. MIT Press.

- [2] D. Alves and J. F. Fontanari. Error threshold in finite populations. *Phys. Rev. E*, 57:7008–7013, 1998.
- [3] Ellen Baake and Wilfried Gabriel. Biological evolution through mutation, selection and drift: An introductory review. *Ann. Rev. Comp. Phys.*, 7, 1999. in press.
- [4] Lloyd Demetrius, Peter Schuster, and Karl Sigmund. Polynucleotide evolution and branching processes. *Bull. Math. Biol.*, 47:239–262, 1985.
- [5] Bernard Derrida and Luca Peliti. Evolution in a flat fitness landscape. *Bull. Math. Biol.*, 53:355–382, 1991.
- [6] Esteban Domingo, Donna Sabo, Tadatsugu Taniguchi, and Charles Weissmann. Nucleotide sequence heterogeneity of an RNA phage population. *Cell*, 13:735–744, 1978.
- [7] M. Eigen. Selforganization of matter and the evolution of biological macromolecules. *Naturwissenschaften*, 58:465–523, 1971.
- [8] M. Eigen and P. Schuster. *The Hypercycle—A Principle of Natural Self-Organization*. Springer-Verlag, Berlin, 1979.
- [9] Manfred Eigen, John McCaskill, and Peter Schuster. Molecular quasi-species. *J. Phys. Chem.*, 92:6881–6891, 1988.
- [10] Manfred Eigen, John McCaskill, and Peter Schuster. The molecular quasi-species. *Adv. Chem. Phys.*, 75:149–263, 1989.
- [11] Warren J. Ewens. *Mathematical Population Genetics*. Springer-Verlag, New York, 1979.
- [12] B. L. Jones. Selection in systems of self-reproducing macromolecules under the constraint of controlled energy fluxes. *Bull. Math. Biol.*, 41:761–766, 1979.
- [13] B. L. Jones. Some models for election of biological macromolecules with time varying constants. *Bull. Math. Biol.*, 41:849–859, 1979.
- [14] B. L. Jones, R. H. Enns, and S. S. Rangnekar. On the theory of selection of coupled macromolecular systems. *Bull. Math. Biol.*, 38:15–28, 1976.
- [15] Ira Leuthäusser. Statistical mechanics of Eigen’s evolution model. *J. Stat. Phys.*, 48:343–360, 1987.

- [16] J. Maynard Smith. Models of evolution. *Proc. R. Soc. London B*, 219:315–325, 1983.
- [17] J. S. McCaskill. A localization threshold for macromolecular quasispecies from continuously distributed replication rates. *J. Chem. Phys.*, 80:5194, 1984.
- [18] H. J. Muller. The relation of recombination to mutational advance. *Mutat. Res.*, 1:2, 1964.
- [19] Martin Nilsson and Nigel Snoad. Error thresholds on dynamic fitness-landscapes. eprint physics/9904023, 1999.
- [20] Martin Nowak and Peter Schuster. Error thresholds of replication in finite populations—mutation frequencies and the onset of Muller’s ratchet. *J. theor. Biol.*, 137:375–395, 1989.
- [21] C. Ronnewinkel. unpublished, 1999.
- [22] C. Ronnewinkel, C. O. Wilke, and T. Martinetz. Genetic algorithms in time-dependent environments. In *Proceedings of the 2nd Evonet Summerschool*, New York, 1999. Springer-Verlag. in press.
- [23] J. E. Rowe. Cyclic attractors and quasispecies adaptability. In *Proceedings of the 2nd Evonet Summerschool*, New York, 1999. Springer-Verlag. in press.
- [24] J. E. Rowe. Finding attractors for periodic fitness functions. In W. Banzhaf et al., editors, *Proceedings of GECCO 1999*, page 557, San Mateo, 1999. Morgan Kaufmann.
- [25] David S. Rumschitzki. Spectral properties of Eigen evolution matrices. *J. Math. Biol.*, 24:667–680, 1987.
- [26] L. Schmitt and C. L. Nehaniv. The linear geometry of genetic operators with applications to the analysis of genetic drift and genetic algorithms using tournament selection. In C. L. Nehaniv, editor, *Mathematical & Computational Biology: Computational Morphogenesis, Hierarchical Complexity, and Digital Evolution*, Lectures on Mathematics in the Life Sciences, pages 147–166. American Mathematical Society, 1999.
- [27] L. Schmitt, C. L. Nehaniv, and R. H. Fujii. Linear analysis of genetic algorithms. *Theor. Comp. Sci.*, 200:101–134, 1998.
- [28] Peter Schuster and Jörg Swetina. Stationary mutant distributions and evolutionary optimization. *Bull. Math. Biol.*, 50:635–660, 1988.

- [29] Jörg Swetina and Peter Schuster. Self-replication with errors—A model for polynucleotide replication. *Biophys. Chem.*, 16:329–345, 1982.
- [30] P. Tarazona. Error thresholds for molecular quasispecies as phase transitions: From simple landscapes to spin-glass models. *Phys. Rev. E*, 45:6038–6050, 1992.
- [31] Colin J. Thompson and John L. McBride. On Eigen’s theory of self-organization of matter and the evolution of biological macromolecules. *Math. Biosci.*, 21:127–142, 1974.
- [32] Erik van Nimwegen and James P. Crutchfield. Metastable evolutionary dynamics: Crossing fitness barriers or escaping via neutral paths? eprint *adap-org/9907002*, 1999.
- [33] Erik van Nimwegen, James P. Crutchfield, and Melanie Mitchell. Statistical dynamics of the royal road genetic algorithm. *Theoretical Computer Science*, 1997. to appear, SFI working paper 97-04-035.
- [34] Thomas Wiehe, Ellen Baake, and Peter Schuster. Error propagation in reproduction of diploid organisms. *J. theor. Biol.*, 177:1–15, 1995.
- [35] Claus O. Wilke. *Evolutionary Dynamics in Time-Dependent Environments*. Shaker Verlag, Aachen, 1999. PhD thesis Ruhr-Universität Bochum.
- [36] Claus O. Wilke, Christopher Ronnewinkel, and Thomas Martinetz. Molecular evolution in time dependent environments. In Dario Floreano, Jean-Daniel Nicoud, and Francesco Mondada, editors, *Advances in Artificial Life, Proceedings of ECAL’99, Lausanne, Switzerland*, Lecture Notes in Artificial Intelligence, pages 417–421, New York, 1999. Springer-Verlag.
- [37] Y. A. Yakubovich and V. M. Starzhinskii. *Linear Differential Equations with Periodic Coefficients*, volume 1. John Wiley & Sons, New York, 1975.